The Plant Cell, Vol. 23: 2285–2301, June 2011, www.plantcell.org

Transcription Factor–Dependent Chromatin Remodeling at Heat Shock and Copper-Responsive Promoters in *Chlamydomonas reinhardtii* [W] [OA]

Daniela Strenkert, Stefan Schmollinger, Frederik Sommer, Miriam Schulz-Raffelt,[1] and Michael Schroda[2]

Max-Planck-Institut für Molekulare Pflanzenphysiologie, D-14476 Potsdam-Golm, Germany

How transcription factors affect chromatin structure to regulate gene expression in response to changes in environmental conditions is poorly understood in the green lineage. To shed light on this issue, we used chromatin immunoprecipitation and formaldehyde-assisted isolation of regulatory elements to investigate the chromatin structure at target genes of HSF1 and CRR1, key transcriptional regulators of the heat shock and copper starvation responses, respectively, in the unicellular green alga *Chlamydomonas reinhardtii*. Generally, we detected lower nucleosome occupancy, higher levels of histone H3/4 acetylation, and lower levels of histone H3 Lys 4 (H3K4) monomethylation at promoter regions of active genes compared with inactive promoters and transcribed and intergenic regions. Specifically, we find that activated HSF1 and CRR1 transcription factors mediate the acetylation of histones H3/4, nucleosome eviction, remodeling of the H3K4 mono- and dimethylation marks, and transcription initiation/elongation. By this, HSF1 and CRR1 quite individually remodel and activate target promoters that may be inactive and embedded into closed chromatin (*HSP22F*/*CYC6*) or weakly active and embedded into partially opened (*CPX1*) or completely opened chromatin (*HSP70A*/*CRD1*). We also observed HSF1-independent histone H3/4 deacetylation at the *RBCS2* promoter after heat shock, suggesting interplay of specific and presumably more generally acting factors to adapt gene expression to the new requirements of a changing environment.

INTRODUCTION

Living organisms may acclimate to abiotic stress by the up- and downregulation of specific sets of genes. Since chromatin remodeling plays an important role in the regulation of gene expression in all eukaryotes examined to date (Kouzarides, 2007; Li et al., 2007), we are interested in how chromatin remodeling affects gene expression in plant systems as a consequence of changes in environmental conditions. We studied this issue in the unicellular green alga *Chlamydomonas reinhardtii*. *Chlamydomonas* has the advantage that changes in environmental conditions may be homogeneously and instantaneously applied to all cells in a cell culture. Moreover, in contrast with land plants, *Chlamydomonas* cells are not differentiated into different cell types or organized into different tissues. The stress responses on which our studies focus, those permitting acclimation to heat shock and copper deficiency, are well characterized in *Chlamydomonas* and therefore well suited for investigations into transcriptional regulation at the chromatin level (Merchant et al., 2006; Schulz-Raffelt et al., 2007).

The heat shock response is regulated by evolutionarily conserved heat shock transcription factors (HSFs), which are activated by hyperphosphorylation and bind as trimers to *cis*-regulatory motifs known as heat shock elements (HSEs) (Sorger and Pelham, 1988; Sorger and Nelson, 1989). HSEs contain at least three 5′-nGAAn-3′ repeats in alternating orientations and are present in the promoters of heat shock genes in a diverse set of organisms (Pelham, 1982). As deletion of HSEs from the *Chlamydomonas HSP70A* promoter entirely abolishes its heat shock inducibility, HSEs are also clearly indispensable for the regulation of the heat shock response in *Chlamydomonas* (Lodha et al., 2008). *Chlamydomonas* contains a single canonical HSF (HSF1), which possesses all features typical for plant (class A) HSFs and represents a key regulator of the stress response in this alga (Schulz-Raffelt et al., 2007). Like in the yeast *Saccharomyces cerevisiae* (but in contrast with the situation for other organisms), *Chlamydomonas* HSF1 forms trimers constitutively and becomes activated by hyperphosphorylation. The two heat shock genes investigated in this work are *HSP70A* and *HSP22F*. *HSP70A* encodes a cytosolic chaperone, which is constitutively expressed and further induced after heat shock (Müller et al., 1992). *HSP22F* encodes a small heat shock protein that is most likely targeted to the chloroplast (Schroda and Vallon, 2008) and only expressed under stress conditions like heat shock (this work).

The copper response regulator (CRR1) is the key regulator of copper homeostasis in *Chlamydomonas* as it mediates activation and repression of target genes of the copper response pathway. CRR1 contains a plant-specific DNA binding domain named SBP that recognizes defined copper response elements (CuREs) with a 5′-GTAC-3′ core sequence. CRR1 binding to the CuREs within the *CYC6*, *CPX1*, and *CRD1* promoters leads to

[1] Current address: Centre National de la Recherche Scientifique, Unité Mixte de Recherche 6191, Commissariat à l'Energie Atomique et aux Energies Alternatives Cadarache, 13108 Saint-Paul-lez-Durance, France.

[2] Address correspondence to schroda@mpimp-golm.mpg.de.

The author responsible for distribution of materials integral to the findings presented in this article in accordance with the policy described in the Instructions for Authors (www.plantcell.org) is: Michael Schroda (Schroda@mpimp-golm.mpg.de).

[W] Online version contains Web-only data.

[OA] Open Access articles can be viewed online without a subscription.

www.plantcell.org/cgi/doi/10.1105/tpc.111.085266

transcriptional activation of these genes (Quinn and Merchant, 1995; Kropat et al., 2005; Sommer et al., 2010). The *CYC6* gene encodes cytochrome c6 (Merchant and Bogorad, 1986), which substitutes for the copper-containing plastocyanin in photosynthetic electron transport under copper deficiency conditions (Wood, 1978; Merchant and Bogorad, 1987). The *CPX1* gene encodes coprogen oxidase (Quinn et al., 1999), and the *copper response defect1 (CRD1)* gene encodes a plastid-localized putative diiron protein that is required for the synthesis of protochlorophyllide (Moseley et al., 2000; Tottey et al., 2003). Hence, the *CPX1* and *CRD1* gene products both are involved in tetrapyrrole biosynthesis.

Chromatin structure is dictated in large part by posttranslational modifications of the unstructured N termini of histones (Luger, 2003; Kouzarides, 2007). Of the many known histone modifications, several are especially intensely studied because they are consistently associated with increased or reduced levels of transcription. These include acetylation of histone H3 at Lys-9 and -14, of histone H4 at Lys-5/8/12/16 and methylation of histone H3 at Lys-4 (Li et al., 2007).

Histone Lys acetylation is mediated by histone acetyltransferases, which in turn are recruited by transcription factors that bind to *cis*-regulatory elements on the underlying DNA (de la Cruz et al., 2005). Histone acetylation again may be recognized by proteins containing bromodomains (Owen et al., 2000) or tandem PHD fingers (Zeng et al., 2010) that may themselves be histone acetyltransferases, factors with ATP-dependent chromatin remodeling activity like SNF2 or Brahma, or components of chromatin remodeling complexes like CHRAC, SAGA, or RSC (Aalfs and Kingston, 2000).

Methyl marks are deposited by methyl-transferases that may, for example, be recruited by the Ser5-phosphorylated RNA polymerase II to target methylation of nucleosomes at the 5′ ends of active genes (Krogan et al., 2003; Ng et al., 2003). Lys methylation is recognized by proteins containing chromodomains, WD40 repeats, or PHD fingers via aromatic cages, which allow discriminating between mono-, di-, and trimethylated lysines (Couture et al., 2006; Li et al., 2006; Ruthenburg et al., 2006). ING2 (inhibitor of growth) is an example of a protein that harbors a PHD finger that recognizes trimethylated Lys-4 at histone H3, which is typically present at promoters of highly transcribed genes (Peña et al., 2006). ING2 in turn may recruit the mSin3a-histone deacetylase complex to repress active genes in response to DNA damage (Shi et al., 2006).

With the goal of determining the relationship between chromatin state and transcriptional activation of heat shock and copper-regulated genes in *Chlamydomonas*, we monitored transcription factor binding, nucleosome occupancy, and levels of histone H3/4 acetylation and histone H3 Lys 4 (H3K4) mono- and dimethylation at heat shock and copper-regulated genes using chromatin immunoprecipitation (ChIP), while in parallel monitoring changes in RNA abundance by quantitative real-time RT-PCR (qRT-PCR). The gene encoding the small subunit of ribulose-1,5-bisphosphate carboxylase/oxygenase 2 (RBCS2) was included as control. We also used formaldehyde-assisted isolation of regulatory elements (FAIRE) (Giresi et al., 2007) to obtain additional information concerning the chromatin state under different environmental conditions. Combined, these approaches provided us with insights into the underlying mechanisms of chromatin remodeling preceding transcriptional activation in *Chlamydomonas*.

RESULTS

HSF1 Is Required for Target Gene Activation by Heat Shock

To study the role of the HSF1 transcription factor in regulating chromatin structure at its target genes, we needed *hsf1* mutant strains. As a stable *hsf1* knockout mutant is not available, we generated strains that are downregulated for HSF1 using RNA interference (RNAi) and artificial microRNA (amiRNA) approaches as described previously (Schulz-Raffelt et al., 2007; Schmollinger et al., 2010). *HSF1*-RNAi and *HSF1*-amiRNA strains were both selected on the basis of thermosensitivity and therefore contained similarly low levels of residual HSF1 protein (Figure 1A; see Supplemental Figure 1A online). As expected, the downregulation of HSF1 strongly impaired but did not entirely abolish the transcription of HSF1 target genes under heat stress: compared with control strains, heat shock–induced transcript accumulation for *HSP70A*, *HSF1*, and *HSP22F* in these lines was reduced on average from ~6.5-fold to ~2.5-fold, ~16-fold to ~2.7-fold, and ~840-fold to ~6.6-fold, respectively (Figure 1B; see Supplemental Figure 1B online). Heat shock had no effect on the accumulation of *RBCS2* and *CYC6* transcripts in control and HSF1-underexpressing lines (Figure 1B).

HSF1 Binds to the Control Regions of the *HSP70A* and *HSP22F* Promoters

To characterize the interaction of HSF1 with its predicted target promoters, we performed ChIP assays on control and *HSF1*-RNAi/amiRNA lines with an affinity-purified polyclonal antiserum against HSF1 (Schulz-Raffelt et al., 2007; see Supplemental Figures 2A and 2B online). Reduced HSF1 accumulation in cells used for ChIP was verified prior to each experiment (Figure 1A). The amounts of precipitated DNA fragments from the *HSP70A*, *HSP22F*, *RBCS2*, and *CYC6* promoters were subsequently quantified by quantitative real-time PCR (qPCR); the amplified regions of the genes are summarized in Figure 2. The specificity of the ChIPs was verified by comparing signals obtained with antibodies against HSF1 with those obtained with antibodies against VIPP2 as a control (see Supplemental Figures 2C and 2D online). In control strains, under nonstress conditions, ChIP with HSF1 antibodies enriched the *HSP70A* and *HSP22F* promoter fragments ~3.4- and ~2-fold, respectively, compared with the *RBCS2* and *CYC6* promoters (Figure 3). Heat shock led to ~13.3- and ~8-fold enrichments of *HSP70A* and *HSP22F* promoter fragments, respectively, compared with *RBCS2* and *CYC6* promoters. Under nonstress conditions, ~1.6 times less *HSP70A* promoter fragments was precipitated from *HSF1*-RNAi/amiRNA strains compared with the control strain, while no change was observed in the amount of precipitated *HSP22F* promoter fragments. Under heat shock conditions, ~3-fold less *HSP70A* promoter fragments was precipitated in *HSF1*-RNAi/amiRNA strains compared with the control strain and enrichment

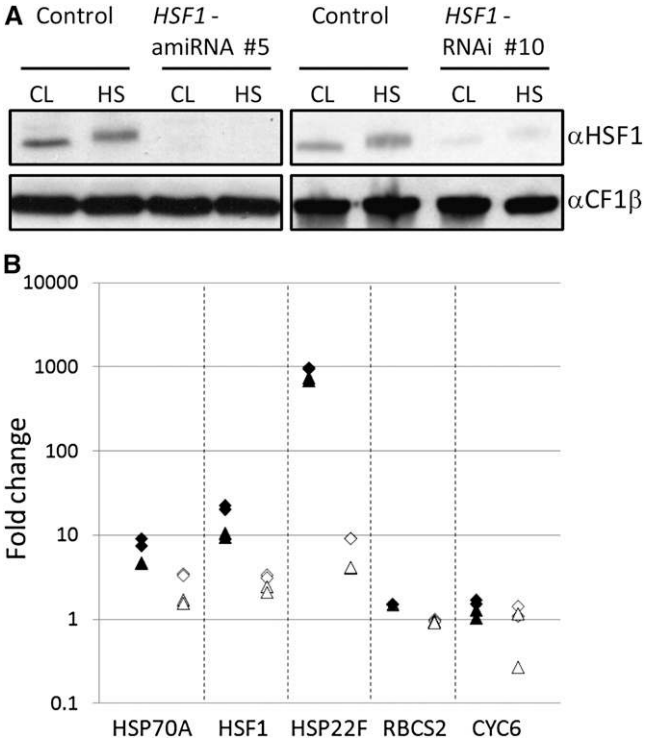

Figure 1. Analysis of Protein and Transcript Levels in HSF1-Underexpressing Strains Prior to ChIP Analysis.

(A) HSF1 abundance is reduced in *HSF1*-amiRNA and -RNAi strains. Control, *HSF1*-amiRNA, and *HSF1*-RNAi lines were kept under nonstress conditions (CL) or subjected to heat shock (HS) for 30 min. Whole-cell proteins were extracted, and proteins corresponding to 2 μg chlorophyll were separated by SDS-PAGE and analyzed by immunoblotting using antisera against HSF1 and CF1β (as loading control).

(B) Accumulation of selected transcripts in control and *HSF1*-RNAi/amiRNA cells. RNA was extracted from nonstressed cells and cells subjected to a 30-min heat shock for analysis by qRT-PCR using the comparative CT method with *CBLP2* as control gene. Primer efficiencies and qRT-PCR end products (amplicons) for all target transcripts are presented in Supplemental Figure 3 online. Shown are fold changes in transcript accumulation between stressed versus nonstressed conditions in control (black) and *HSF1*-RNAi/amiRNA lines (white), respectively. Three technical replicates each from *HSF1*-RNAi line #10 (triangles) and *HSF1*-amiRNA line #5 (diamonds) were performed.

of *HSP22F* promoter fragments was completely abolished. These data suggest that HSF1 constitutively binds to the *HSP70A* promoter, but not the *HSP22F* promoter, and that binding at both promoters increases ~4-fold during heat stress. Moreover, HSF1 appears to have a higher affinity for the *HSP70A* promoter than for the *HSP22F* promoter, as judged from the binding of residual HSF1 to *HSP70A* but not to *HSP22F* in *HSF1*-RNAi/amiRNA strains.

HSF1 Appears to Be Responsible for Nucleosome Remodeling

To analyze whether HSF1 affects nucleosome occupancy at its target promoters, we performed ChIP with antibodies against the C terminus of core histone H3, which is known not to be modified. For a better comparability of biological replicates, we normalized values resulting from qPCR quantification of precipitated DNA fragments relative to those obtained for amplification of 10% input DNA and to the values obtained for the *CYC6* promoter. The *CYC6* promoter is inactive in the presence of copper (Quinn and Merchant, 1995), which explains why heat shock had no effect on mRNA expression, nucleosome occupancy, or histone modifications at *CYC6* (Figure 1B; see Supplemental Figures 4B and 5A online).

In nonstressed control cells, nucleosome occupancy at the heat shock gene promoters was 30 to 50% lower than at the *CYC6* promoter. Heat shock led to a further reduction of nucleosome occupancy by ~1.6-fold at the *HSP22F* promoter and by ~10-fold at the *HSP70A* promoter (Figure 4A; see Supplemental Figure 4A online). The latter result was consistent with the observation that much lower levels of *HSP70A* promoter fragments were precipitated with antibodies against modified histones from heat shock samples compared with nonstressed controls (see below). In the *HSF1*-RNAi/amiRNA strains, we observed the same ~10-fold reduction of nucleosome occupancy at the *HSP70A* promoter after heat shock as seen in the control strain, whereas the reduction of nucleosome occupancy at the *HSP22F* promoter was less pronounced. This suggested

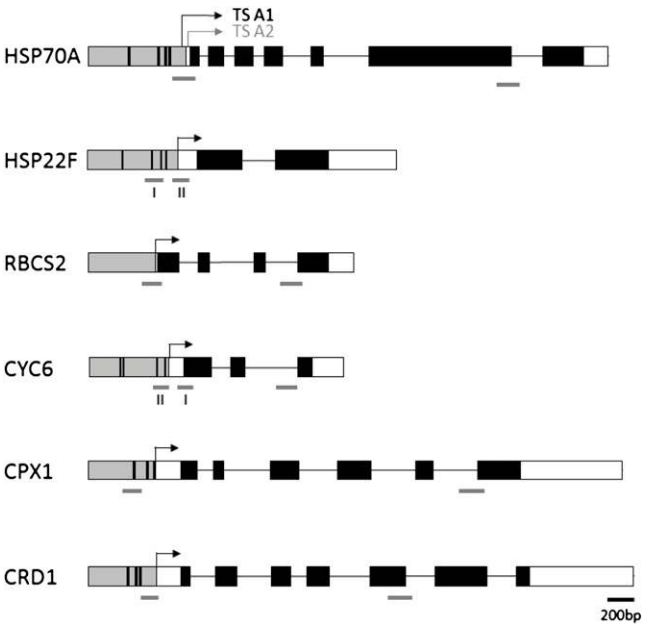

Figure 2. Regions Amplified from Chromatin Immunoprecipitates by qPCR.

Shown are the six genes investigated in this study. Promoter regions are indicated by gray boxes, transcriptional start sites (TS) by arrows, translated regions by black boxes, untranslated regions by white boxes, and introns by thin lines. The *HSP70A* promoter has two transcriptional start sites designated TSA1 and TSA2 (von Gromoff et al., 2006). Vertical black lines designate putative HSEs in the *HSP70A* and *HSP22F* promoter regions and putative CuREs in the *CYC6*, *CPX1*, and *CRD1* promoters. Gray bars designate the regions amplified by qPCR (if not indicated otherwise, region I was used by default for *HSP22F* and *CYC6*).

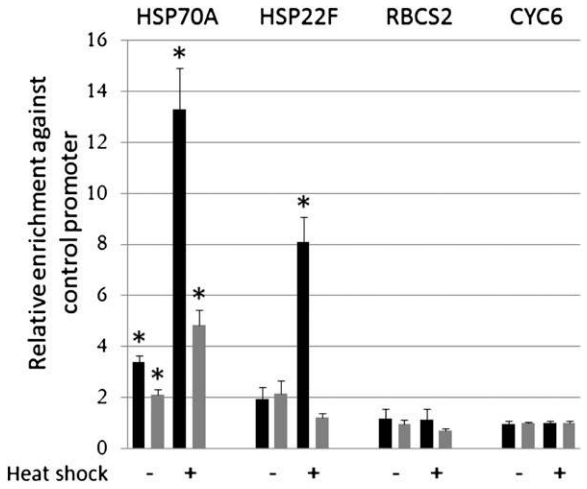

Figure 3. HSF1 Binds to Promoters *HSP70A* and *HSP22F*.

ChIP was done on control (black bars) and HSF1-underexpressing strains (gray bars) grown under nonstress conditions or subjected to a 30-min heat shock. From DNA fragments precipitated with αHSF1 antibodies the promoter regions shown in Figure 2 were amplified by qPCR. The enrichment relative to 10% input DNA was calculated and normalized to the values obtained for the *CYC6* promoter. Error bars indicate standard errors of the mean of two biological replicates, with each analyzed in triplicate. HSF1-underexpressing strains analyzed were *HSF1*-RNAi line #10 and *HSF1*-amiRNA line #5. Asterisks indicate the significance of change compared with the *CYC6* promoter in control cells under nonstress conditions (*t* test, P value ≤ 0.01).

that HSF1 was to some extent responsible for reducing nucleosome occupancy at the *HSP22F* promoter. This may be true also for the *HSP70A* promoter but might be concealed by its higher affinity for HSF1, leading to binding of the residual HSF1 present in *HSF1*-RNAi/amiRNA strains (Figure 3).

Interestingly, nucleosome occupancy at the *RBCS2* promoter increased by ~20% after heat shock (Figure 4A). As this effect was observed equally in control and *HSF1*-RNAi/amiRNA strains, it appears to be independent of HSF1.

HSF1 Promotes Increased Levels of Histone H3/H4 Acetylation at Heat Shock Gene Promoters

The levels of histone H3 and H4 acetylation and the methylation state of Lys-4 (K4) at histone H3 are known to be crucial marks for the regulation of euchromatic genes. Hence, we wanted to determine whether HSF1 binding to the heat shock gene promoters influences levels of H3/4 acetylation and H3K4 mono- and dimethylation of local nucleosomes. We first performed ChIP analyses using antibodies against di-acetylated histone H3 and tetra-acetylated histone H4. We chose to generally express histone modifications (e.g., Figure 4B) relative to the abundance of nucleosomes at the DNA fragment investigated (Figure 4A) to account for variations in nucleosome occupancy.

Strikingly, in control cells, histone H3 was acetylated at ~14-fold higher levels at the *HSP70A* promoter than at the *CYC6* promoter (Figure 4B). Although the low nucleosome occupancy of the *HSP70A* promoter during heat shock makes correct quantification of histone modifications difficult, H3 acetylation levels appeared to be equally high under nonstress and stress conditions. By contrast, histone H3 acetylation levels at the *HSP70A* promoter were ~35 to 50% lower in *HSF1*-RNAi/amiRNA strains under nonstress and stress conditions, thus pointing to a role of HSF1 in promoting histone H3 acetylation. In contrast with the *HSP70A* promoter, histone H3 acetylation levels at the *HSP22F* promoter under nonstress conditions were only slightly elevated when compared with the *CYC6* promoter. Levels of H3 acetylation at the *HSP22F* promoter were the same in control cells as in the *HSF1*-RNAi/amiRNA strains under nonstress conditions but increased more than 3-fold in the control strain following heat shock, while they did not increase at all in the *HSF1*-RNAi/amiRNA strains. Again, these results point to a role of HSF1 in promoting H3 acetylation at heat shock gene promoters. Histone H3 acetylation levels at the *RBCS2* promoter were ~4-fold higher than at the *CYC6* promoter and tended to decline during heat shock. As the effect was similar in control and *HSF1*-RNAi/amiRNA strains, it appears to be HSF1 independent.

ChIP analyses using antibodies against acetylated H4 yielded similar results. In control cells under nonstress conditions, histone H4 at the *HSP70A* promoter was acetylated at ~10-fold higher levels than histone H4 at the *CYC6* promoter (Figure 4C). Although difficult to assess accurately, levels of H4 acetylation of the few nucleosomes remaining on *HSP70A* promoter fragments tended to increase even more during heat shock. This tendency was not observed in *HSF1*-RNAi/amiRNA strains, thus suggesting a role of HSF1 also in promoting H4 acetylation. In control cells, histone H4 acetylation levels at the *HSP22F* promoter were ~2- and ~16-fold higher than at the *CYC6* promoter during nonstress and heat shock conditions, respectively (Figure 4C). By contrast, in *HSF1*-RNAi/amiRNA strains under nonstress conditions, H4 acetylation levels at the *HSP22F* promoter were as low as at the *CYC6* promoter, and during stress, they were only ~7-fold higher, supporting the conclusion that HSF1 is required for H4 acetylation at the heat shock gene promoters. Under nonstress conditions, histone H4 acetylation levels at the *RBCS2* promoter were even ~6-fold higher than at the *CYC6* promoter, but during heat shock dropped to the same low levels as at the *CYC6* promoter. Since this effect was observed in both control and *HSF1*-RNAi/amiRNA strains, it appears to be HSF1 independent.

Under nonstress conditions, histone H3K4 dimethylation levels at the *CYC6* and *HSP22F* promoters were comparable, whereas they were ~3- and ~8-fold lower at the *HSP70A* and *RBCS2* promoters than at *CYC6*, respectively (Figure 4D). Heat shock appeared to result in an ~2.7-fold increase in H3K4 dimethylation levels at the *HSP70A* promoter; however, given the low nucleosome occupancy at the *HSP70A* promoter during heat shock, this observation may not be meaningful. In control cells, H3K4 monomethylation levels were comparable at promoters *CYC6*, *HSP22F*, and *RBCS2* under nonstress and heat shock conditions (Figure 4E). By contrast, H3K4 monomethylation was ~6-fold lower at the *HSP70A* promoter than at *CYC6* under nonstress conditions but seemed to increase ~4-fold during heat shock. As for dimethylation of H3K4, this result might not be

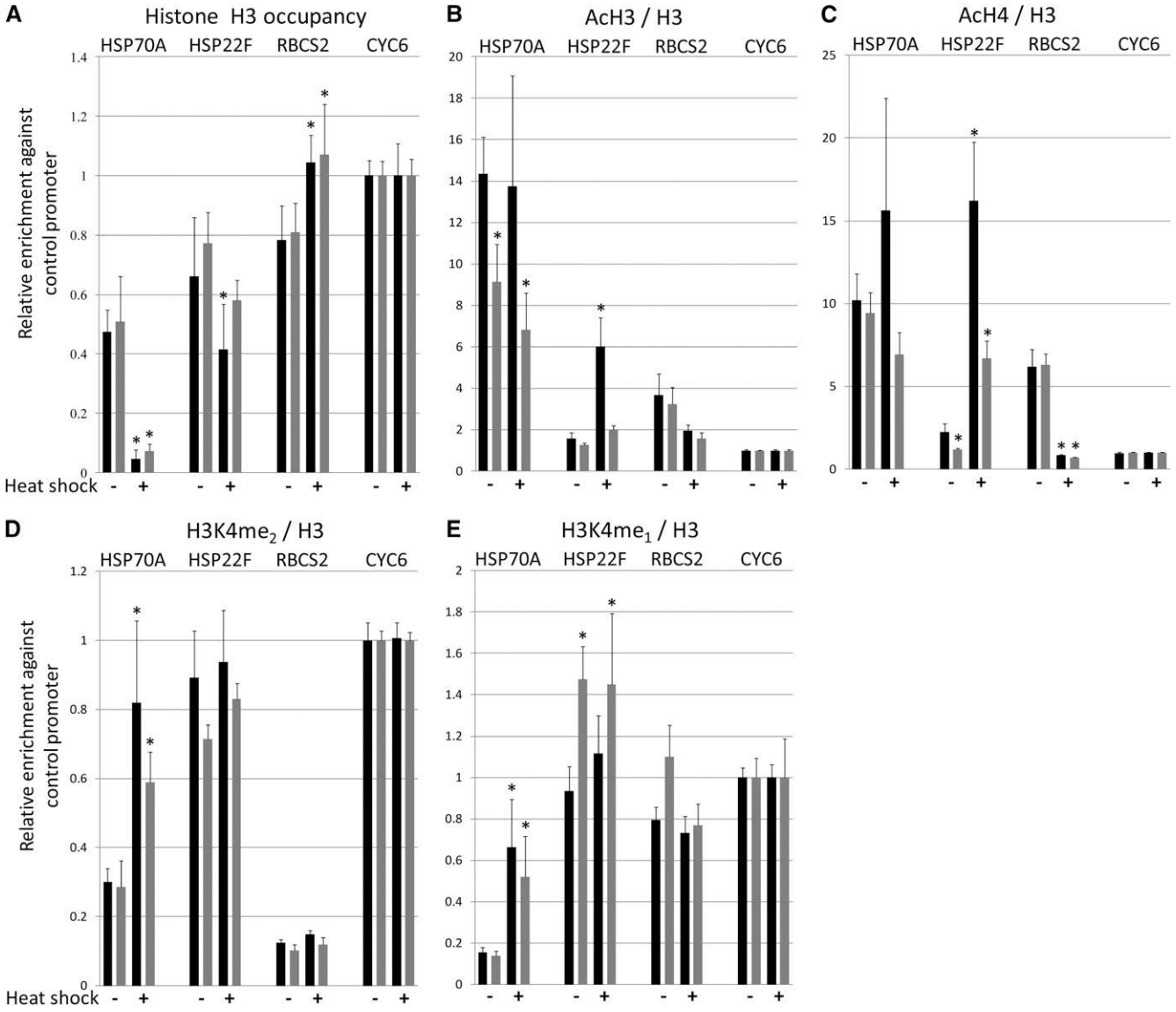

Figure 4. Analysis of Nucleosome Occupancy and Histone Modifications at Heat Shock–Responsive and Control Promoters.

(A) Nucleosome occupancy declines at heat shock gene promoters after heat shock. ChIP was done as described in Figure 3 but using antibodies against the unmodified C terminus of histone H3 to determine nucleosome occupancy at the indicated promoters in control (black bars) and HSF1-underexpressing strains (gray bars).

(B) HSF1 promotes acetylation of histone H3 at the *HSP70A* and *HSP22F* promoters. ChIP was done using antibodies against acetylated Lys-9 and -14 of histone H3.

(C) HSF1 promotes acetylation of histone H4 at the *HSP22F* promoter. ChIP was done using antibodies against acetylated Lys-5, -8, -12, and -16 of histone H4.

(D) HSF1 has no effect on histone H3 dimethylation at the heat shock gene promoters. ChIP was done using antibodies against dimethylated Lys-4 at histone 3 (H3K4).

(E) HSF1 might reduce histone H3 monomethylation at the *HSP22F* promoter. ChIP was done using antibodies against monomethylated Lys-4 at histone 3 (H3K4).

qPCR data from the experiments in **(B)** to **(E)** are given relative to the nucleosome occupancy at the respective promoter region (data from **[A]**). Error bars indicate standard errors of the mean of two biological replicates, with each analyzed in triplicate. Asterisks indicate the significance of change at the respective promoter compared with control cells under nonstress conditions (*t* test, P value ≤ 0.05).

meaningful because few nucleosomes remain on *HSP70A* promoter fragments under heat shock conditions. While the same patterns of H3K4 dimethylation were observed in control and *HSF1*-RNAi/amiRNA strains and therefore appeared not to depend on HSF1, levels of H3K4 monomethylation were higher at the *HSP22F* promoter under nonstress and stress conditions in the *hsf1* mutant compared with control cells. This suggests that HSF1 might be responsible for the reduced levels of monomethylation at the *HSP22F* promoter.

HSF1 Binding at the *HSP22F* Promoter Precedes Histone Acetylation/Eviction and Transcriptional Activation

To gain mechanistic insights into how transcriptional activation by HSF1 is mediated in *Chlamydomonas*, it is necessary to resolve when exactly after onset of heat stress the processes of transcription factor binding, histone modification, histone eviction, and transcription take place. Under nonstress conditions, the *HSP22F* gene is not transcribed, HSF1 does not bind to the promoter, nucleosome occupancy is relatively high, and histones H3 and H4 contain low levels of acetylation (Figures 3 and 4; see Supplemental Figure 2D online). Hence, the *HSP22F* gene appears to be an ideal target to study the sequence of events leading to transcriptional activation by heat stress. To this end, we performed a time-course analysis of HSF1 binding, histone occupancy, and histone H3/4 acetylation at the *HSP22F* promoter and of *HSP22F* mRNA accumulation within the first 10 min after exposing control cells to heat stress. This analysis revealed that occupation of the *HSP22F* promoter by HSF1 is detectable already 30 s after the onset of heat shock, which correlates with an ~2-fold increase in levels of histone H4 acetylation (Figure 5). Within 60 s after onset of heat stress, HSF1 has already reached ~30% of its maximal occupancy at the *HSP22F* promoter and acetylation levels of histones H3 and H4 have increased ~2- and ~5.6-fold, respectively, which coincides with a reduction of histone occupancy by ~35%. Note that almost identical results were obtained when a region located at the *HSP22F* transcriptional start site rather than at the HSEs was amplified from chromatin precipitates (region II of *HSP22F* in Figure 2; see Supplemental Figure 6A online). As a strong increase in *HSP22F* transcript levels was detected only 2 min after onset of heat stress, nucleosome remodeling at the *HSP22F* promoter is more likely a prerequisite for rather than a consequence of transcription.

Nucleosome Remodeling at Promoters of Copper-Responsive Genes Depends on CRR1

To elucidate whether our results from HSF1-mediated chromatin remodeling at heat shock promoters can more generally be applied to other *Chlamydomonas* promoters responsive to changes in environmental conditions, we extended our studies to the copper response. In contrast with the situation for HSF1, a mutant harboring a stable knockout of the gene encoding the key regulator of copper homeostasis, CRR1, is available (Eriksson et al., 2004). As expected, the induction of CRR1 target genes *CYC6*, *CPX1*, and *CRD1* after copper depletion was entirely abolished in the *crr1* knockout mutant (Figure 6), hence corroborating the results reported previously by Kropat et al. (2005). The variation in CRR1 target gene expression levels in control (*CRR1*$^+$) cells under copper-depleted conditions is due to slight variations in residual copper ion concentrations in the cell cultures.

As we were not able to immunoprecipitate native or green fluorescent protein–tagged CRR1, we could not directly test for preloading of copper-responsive promoters by CRR1. Hence, we had to limit our analysis to the investigation of nucleosome occupancy and histone modifications in control and *crr1* mutant strains under copper-replete and copper deprivation conditions. This time, we normalized qPCR quantification values relative to those obtained for the *RBCS2* promoter, whose associated expression levels, nucleosome occupancy, and histone modifications remained unaffected by copper starvation (see Supplemental Figure 5B online). In control and *crr1* mutant cells, nucleosome occupancy under copper-replete conditions was similar between the *CYC6* and *RBCS2* promoters, whereas it was 40 to 60% lower at the *CPX1* and *CRD1* promoters (Figure 7A). In control cells, copper depletion led to a 1.3- to 2-fold reduction of nucleosome occupancy at the *CYC6*, *CPX1*, and *CRD1* promoters, whereas no such effect was observed in *crr1* mutant cells. These results suggest that, similar to what was observed for HSF1 at the *HSP22F* promoter, CRR1 appeared to be responsible for reducing nucleosome occupancy at copper-responsive promoters.

CRR1 Promotes Higher Levels of Histone H3/H4 Acetylation and Lower Levels of H3K4 Mono- and Dimethylation at the *CYC6* and *CPX1* Promoters

We next asked whether CRR1, like HSF1, promotes histone acetylation at its target promoters. As shown in Figure 7B, this is indeed the case for some targets: in control cells, after copper depletion, H3 acetylation increased at the *CYC6* and *CPX1* promoters by factors of ~4 and ~1.6, respectively, whereas this effect was not observed in the *crr1* mutant. No changes in histone H3 acetylation levels were observed at the *CRD1* promoter. Interestingly, under copper-replete conditions, H3 acetylation levels were ~2-fold lower at the *CYC6* promoter than at the *RBCS2* promoter, whereas they were ~1.5- and 2.5-fold higher at the *CPX1* and the *CRD1* promoters, respectively, than at *RBCS2*.

A similar picture was obtained for H4 acetylation. Here, under copper-replete conditions, acetylation levels at the *CYC6* and *CPX1* promoters were ~6- and ~3-fold lower, respectively, than at the *RBCS2* promoter. After copper depletion, however, H4 acetylation at *CYC6* and *CPX1* increased more than 8-fold relative to copper-replete conditions (Figure 7C). This effect was not observed in the *crr1* mutant, indicating that H4 acetylation of nucleosomes at the *CYC6* and *CPX1* gene promoters is mediated by the CRR1 transcription factor. Histone H4 acetylation at the *CRD1* promoter was independent of both copper availability and CRR1: in all strains and under all conditions tested, it was ~2.5-fold higher than at the *RBCS2* promoter.

To get an estimate on how much the region that was chosen within the target promoter for amplification from chromatin immunoprecipitates influenced the results, we analyzed nucleosome occupancy and H3/4 acetylation at a different region of the *CYC6* promoter in control and *crr1* mutant cells under

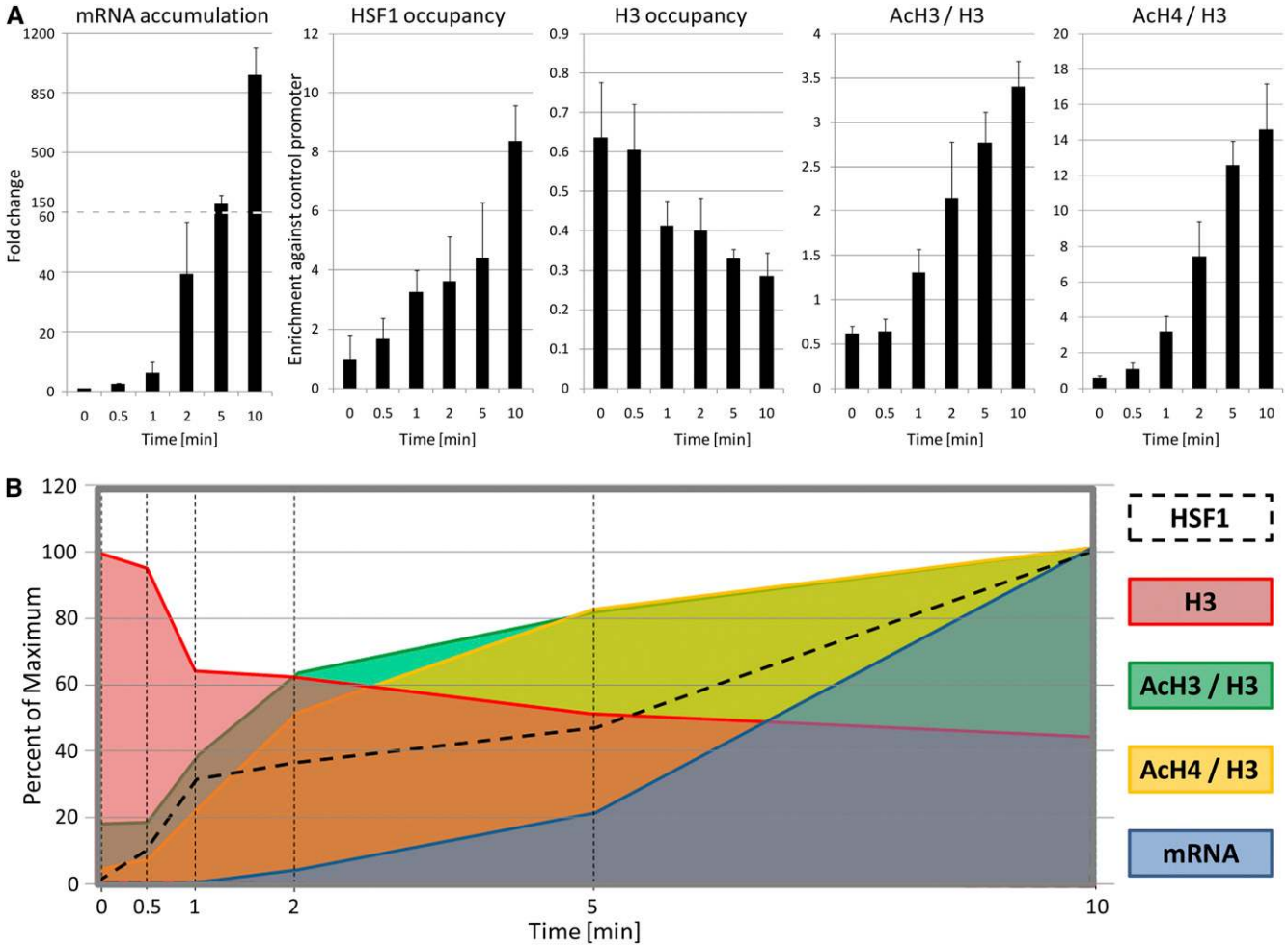

Figure 5. Analysis of the Sequence of Events at the *HSP22F* Promoter within the First 10 min after Onset of Heat Stress.

(A) HSF1 binding precedes chromatin remodeling and transcription. Control cells were subjected to heat stress, and samples for RNA extraction and ChIP were taken immediately prior to the temperature shift and at the indicated time points after shift from 25 to 40°C. *HSP22F* mRNA levels were quantified by qRT-PCR as described in Figure 1B. Shown are fold changes in transcript accumulation relative to the nonstressed state. Values derive from two biological replicates, with each analyzed in triplicate. ChIP was done as described in Figure 3, again amplifying region I of the *HSP22F* promoter (Figure 2). The enrichment relative to 10% input DNA was calculated and normalized to the values obtained for the *CYC6* promoter. Error bars indicate standard errors of two biological replicates, each analyzed in triplicate.

(B) Graphical overview of the sequence of events at the *HSP22F* promoter after onset of heat stress. The data from **(A)** are given as percentage of the respective maximal values.

copper-replete conditions and after copper depletion (region II of the *CYC6* promoter in Figure 2). While histone occupancy was ~1.7-fold higher within the *CYC6* 5′ untranslated region (region I) than at the relevant copper-responsive elements (region II), CRR1-dependent reduction in nucleosome occupancy and relative increases in H3/4 acetylation were the same at both regions (see Supplemental Figure 6B online). Combined with the results obtained for the two different regions analyzed within the *HSP22F* promoter (Figure 2; see Supplemental Figure 6A online), these data indicate that the chromatin state at the actual promoter regions appears to spread into the flanking regions.

Under copper-replete conditions, the *CYC6* and *CPX1* promoters are associated with 7- to 8-fold higher levels of histone H3K4 dimethylation than the *RBCS2* promoter, and the *CRD1* promoter possesses ~2.5-fold higher levels than *RBCS2* (Figure 7D). At the *CYC6* and *CPX1* promoters, H3K4 dimethylation levels decreased ~2-fold in response to copper depletion. This effect was not as pronounced in the *crr1* mutant, suggesting a role for the CRR1 transcription factor in mediating remodeling of the dimethylation mark. H3K4 dimethylation levels at the *CRD1* promoter were the same regardless of copper or CRR1 availability.

Under copper-replete conditions, levels of histone H3K4 monomethylation were ~2.5-fold higher at the *CYC6* promoter than at the *RBCS2* promoter but ~2-fold lower at the *CPX1* and *CRD1* promoters than at *RBCS2* (Figure 7E). Interestingly, in

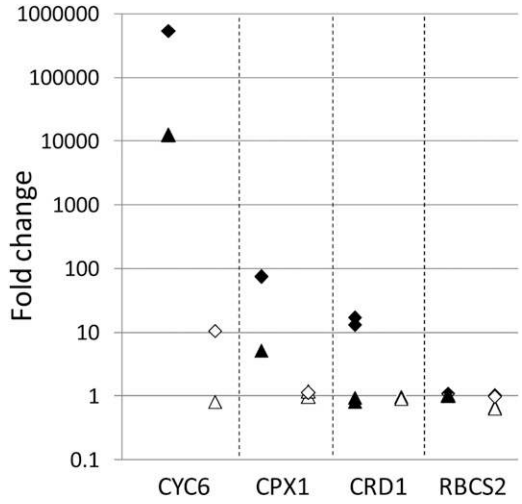

Figure 6. Accumulation of Selected Transcripts in Control and *crr1* Mutant Cells.

Transcript accumulation in copper-replete versus copper-deprived control (black) and *crr1* mutant cells (white) was assessed by qRT-PCR as described in Figure 1B. Values shown are from two biological replicates (triangles and diamonds), each analyzed in triplicate.

response to copper depletion, H3K4 monomethylation levels decreased by a factor of ~10 at the *CYC6* promoter and by a factor of ~2 at the *CPX1* and *CRD1* promoters. These effects were largely abolished in the *crr1* mutant, suggesting that CRR1 also plays a role in remodeling of the H3K4 monomethylation mark.

FAIRE Analysis Indicates That Transcription Factor–Mediated Chromatin Remodeling Occurs at Target Promoters

Our ChIP results suggest that the HSF1 and CRR1 transcription factors under inducing conditions mediate chromatin remodeling toward an open chromatin structure at the heat shock and copper-responsive promoters, respectively. To test this conclusion using a second assay, we employed the FAIRE technique. FAIRE is a non-antibody-based method that involves formaldehyde cross-linking of DNA-protein complexes and that enriches for DNA fragments that correspond to regions of open chromatin structure (Giresi et al., 2007).

As shown in Figure 8A, ~2.5 times more *HSP70A* than *HSP22F* promoter fragments were enriched by FAIRE (relative to input DNA) in nonstressed cells, indicating that the *HSP70A* promoter is constitutively in a more open conformation than the *HSP22F* promoter. Furthermore, enrichment of *HSP70A* and *HSP22F* promoter fragments was ~1.5- and ~2-fold greater, respectively, for control cells subjected to heat shock relative to nonstressed cells, while there was no enrichment for *HSP22F* promoter fragments in heat-shocked *HSF1*-amiRNA cells, relative to nonstressed cells. Interestingly, in control and *crr1* mutant cells grown under copper-replete conditions, roughly the same quantity of *CYC6*, *CPX1*, and *CRD1* promoter fragments were enriched by FAIRE (Figure 8B), and these amounts were comparable to those obtained for the inactive *HSP22F* promoter (Figure 8A). Copper depletion led to a 1.6- to 2-fold increase in FAIRE-enriched fragments of the *CYC6*, *CPX1*, and *CRD1* promoters, but there was no enrichment of these promoter fragments in *crr1* mutant cells (Figure 8B). When compared with ChIP, FAIRE indicated a more pronounced opening of chromatin structure at the *CRD1* promoter in copper-depleted control cells (cf. Figures 7A and 8B). This might be explained by the comparably low sensitivity of the *CRD1* gene to copper depletion (Figure 6), which might prevent a clearer detection of changes in nucleosome occupancy. Overall, the data obtained from these FAIRE experiments corroborate the ChIP results reported above, namely, that HSF1 and CRR1 transcription factors mediate chromatin remodeling at their target promoters.

Gene-Wide Analysis of the Distribution of Chromatin Marks

To gain insights into general aspects of chromatin organization in *Chlamydomonas*, we compared the distribution of chromatin marks throughout representative parts of the six genes analyzed in this study, including promoter, transcribed, and two intergenic regions (see Figure 2 for promoter and transcribed regions assayed). As a general trend, we observed lower histone occupancy, higher levels of histone H3/4 acetylation, and lower levels of H3K4 monomethylation at promoter regions of active genes compared with levels at inactive promoters and at transcribed and intergenic regions (Figure 9). H3K4 monomethylation appears to be particularly high in the 3′ region of actively transcribed genes. No distinct pattern was observed for H3K4 dimethylation, except for a potential enrichment in promoter regions of inactive genes.

DISCUSSION

We employed the ChIP and FAIRE techniques to study how transcription factors affect chromatin structure to regulate the expression of target genes in response to changes in environmental conditions in *Chlamydomonas*. We focused our analysis on five genes of the heat shock and copper response pathways that in *Chlamydomonas* are regulated by the HSF1 and CRR1 transcription factors, respectively. Our results, summarized in Figure 10, reveal that both transcription factors regulate the expression of these genes via conserved mechanisms involving histone acetylation, histone methylation, nucleosome eviction, and polymerase loading/activation. However, at each target promoter, these means are employed quite individually to establish a characteristic chromatin state, presumably to allow for a fine-tuning of gene expression that meets the requirements of the respective environmental condition.

Preloading of Transcription Factors

ChIP assays using antibodies against HSF1 revealed that HSF1 constitutively binds the *HSP70A* promoter and that the association increased ~4-fold after heat shock (Figures 3 and 10; see Supplemental Figure 2D online). This finding is in line with previous findings showing that constitutive hypersensitive sites exist at the HSE1/TATA box and HSE4 within the *HSP70A*

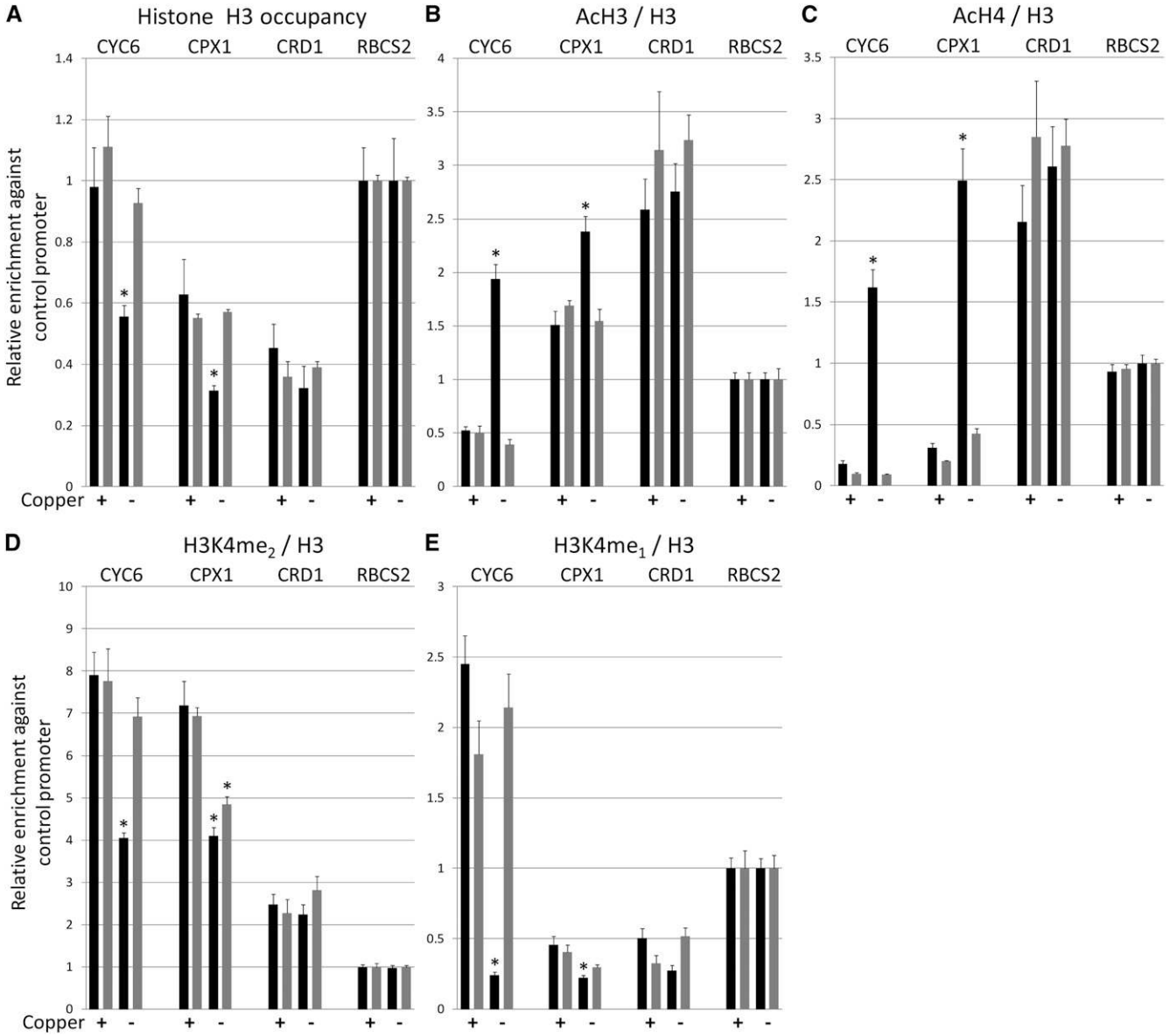

Figure 7. Analysis of Nucleosome Occupancy and Histone Modifications at Copper-Responsive and Control Promoters.

(A) Nucleosome occupancy declines at copper-responsive gene promoters under copper depletion. ChIP was done on control (black bars) and *crr1* knockout cells (gray bars) grown under copper-replete or copper deprivation conditions. From DNA fragments precipitated with antibodies against the unmodified C terminus of histone H3, the promoter regions shown in Figure 2 were amplified by qPCR. The enrichment relative to 10% input DNA was calculated and normalized to the values obtained for the *RBCS2* promoter. Error bars indicate standard errors of two biological replicates, each analyzed in triplicate.

(B) CRR1 promotes histone H3 acetylation at the *CYC6* and *CPX1* promoters after copper depletion. ChIP was done using antibodies against acetylated Lys-9 and -14 of histone H3.

(C) CRR1 promotes histone H4 acetylation at the *CYC6* and *CPX1* promoters after copper depletion. ChIP was done using antibodies against acetylated Lys-5, -8, -12, and -16 of histone H4.

(D) CRR1 promotes reduction of H3K4 dimethylation at promoters *CYC6* and *CPX1* after copper depletion. ChIP was done using antibodies against dimethylation of Lys-4 at histone H3 (H3K4).

(E) CRR1 promotes reduction of H3K4 monomethylation at promoters *CYC6* and *CPX1* after copper depletion. ChIP was done using antibodies against monomethylation of Lys-4 at histone H3 (H3K4).

qPCR data from the experiments in **(B)** to **(E)** are given relative to the nucleosome occupancy at the respective promoter region (data from **[A]**). Asterisks indicate the significance of change at the respective promoter compared with control cells under copper replete conditions (*t* test, P value $\leq$ 0.01).

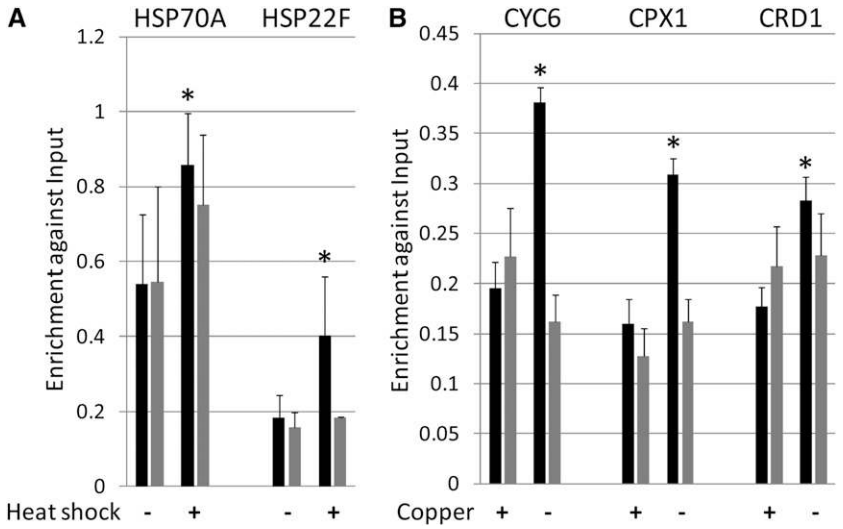

Figure 8. FAIRE Indicates Chromatin Remodeling after Transcriptional Activation.

(A) Nucleosome occupancy declines at heat shock gene promoters after heat shock. FAIRE was performed with control (black bars) and HSF1-underexpressing cells (gray bars) grown under nonstress conditions or subjected to a 30-min heat shock. DNA fragments present in the supernatant after phenol/chloroform extraction of formaldehyde-cross-linked chromatin were precipitated, and the promoter regions of *HSP70A* and *HSP22F* (Figure 2) were amplified by qPCR. The enrichment relative to input DNA, after reversion of the cross-link, was calculated. Error bars indicate standard errors from two biological replicates, each analyzed in duplicate. Asterisks indicate the significance of change at the respective promoter compared with control cells under nonstress conditions (*t* test, P value $\leq$ 0.05).

(B) Nucleosome occupancy declines at the *CYC6* promoter after copper depletion. FAIRE was performed with control and *crr1* knockout cells grown in the presence or absence of copper. qPCR analyses were done as in **(A)**. Asterisks indicate the significance of change at the respective promoter compared with control cells under copper replete conditions (*t* test, P value $\leq$ 0.01).

promoter (Lodha and Schroda, 2005). Constitutive binding to heat shock gene promoters was reported for yeast HSF1, but not for human, fly, or plant HSFs (Sorger et al., 1987; Zhang et al., 2003; Erkina and Erkine, 2006; Kodama et al., 2007). This discrepancy is presumably related to the fact that like yeast HSF1, *Chlamydomonas* HSF1 is constitutively trimeric, but HSF1 trimerization is induced only under stress conditions in higher plants, flies, and humans (Sorger and Nelson, 1989; Rabindran et al., 1993; Lee et al., 1995; Schulz-Raffelt et al., 2007). While HSF1 preloading was evident at the *HSP70A* promoter, little or none was observed at the *HSP22F* promoter (Figures 3, 5, and 10; see Supplemental Figure 2D online). Similar observations were made in yeast, where preloading was observed at the *HSP82* and *SSA4* promoters but not at the *HSP12* promoter (Erkina and Erkine, 2006; Erkina et al., 2010). Apparently, it may be a widespread phenomenon that HSFs occupy small heat shock gene promoters only after stress (Erkina and Erkine, 2006; Kodama et al., 2007), and this generalization correlates well with the expression of many *sHSP* genes only under stress conditions (Haslbeck, 2002).

In the absence of a functional antibody against CRR1, we could not perform ChIP experiments to analyze whether CRR1 binds to its target promoters also in the presence of copper. However, as ChIP and FAIRE analyses revealed no striking differences between the chromatin states of noninduced control and *crr1* mutant strains (Figures 7 and 8), it appears more likely that CRR1 is not preloaded to its target promoters in the presence of copper.

Constitutive versus Inducible Histone Modification

We observed constitutively high levels of histone H3 and H4 acetylation at the *HSP70A* and *CRD1* promoters (Figures 4B, 4C, 7B, 7C, and 10). In HSF1-underexpressing strains, constitutive H3 acetylation at the *HSP70A* promoter was lower and therefore appears to be mediated by preloaded HSF1. On the contrary, as H3/4 acetylation levels at the *CRD1* promoter were constitutively high in control and *crr1* mutant cells, they must be mediated by an activator distinct from CRR1. In contrast with the *HSP70A* and *CRD1* promoters, the *HSP22F*, *CYC6*, and *CPX1* promoters had low levels of H3 and particularly H4 acetylation under noninducing conditions. However, levels of acetylation increased under heat shock (*HSP22F*) or copper deprivation (*CYC6* and *CPX1*) conditions. Inducible H3/4 acetylation at these promoters appears to be mediated by HSF1 and CRR1, as it was reduced or abolished in the respective mutant strains (Figures 4B, 4C, 7B, 7C, and 10; see Supplemental Figure 6B online). A direct role for HSF1 in mediating histone acetylation at target promoters has also been demonstrated in yeast by the use of strains carrying a mutated HSE (Zhao et al., 2005) or expressing an HSF1 variant without transactivation domain (Erkina and Erkine, 2006). Good candidates for coactivators of *Chlamydomonas* HSF1 with histone acetylase activity are homologs of the yeast NuA4 and SAGA complexes that, following heat shock, have been shown to rapidly enrich at HSF1-dependent heat shock gene promoters (Reid et al., 2000; Robert et al., 2004; Kremer and Gross, 2009). In contrast with *Chlamydomonas*, it is not clear whether preloaded HSF1 also drives constitutive histone acetylation in yeast.

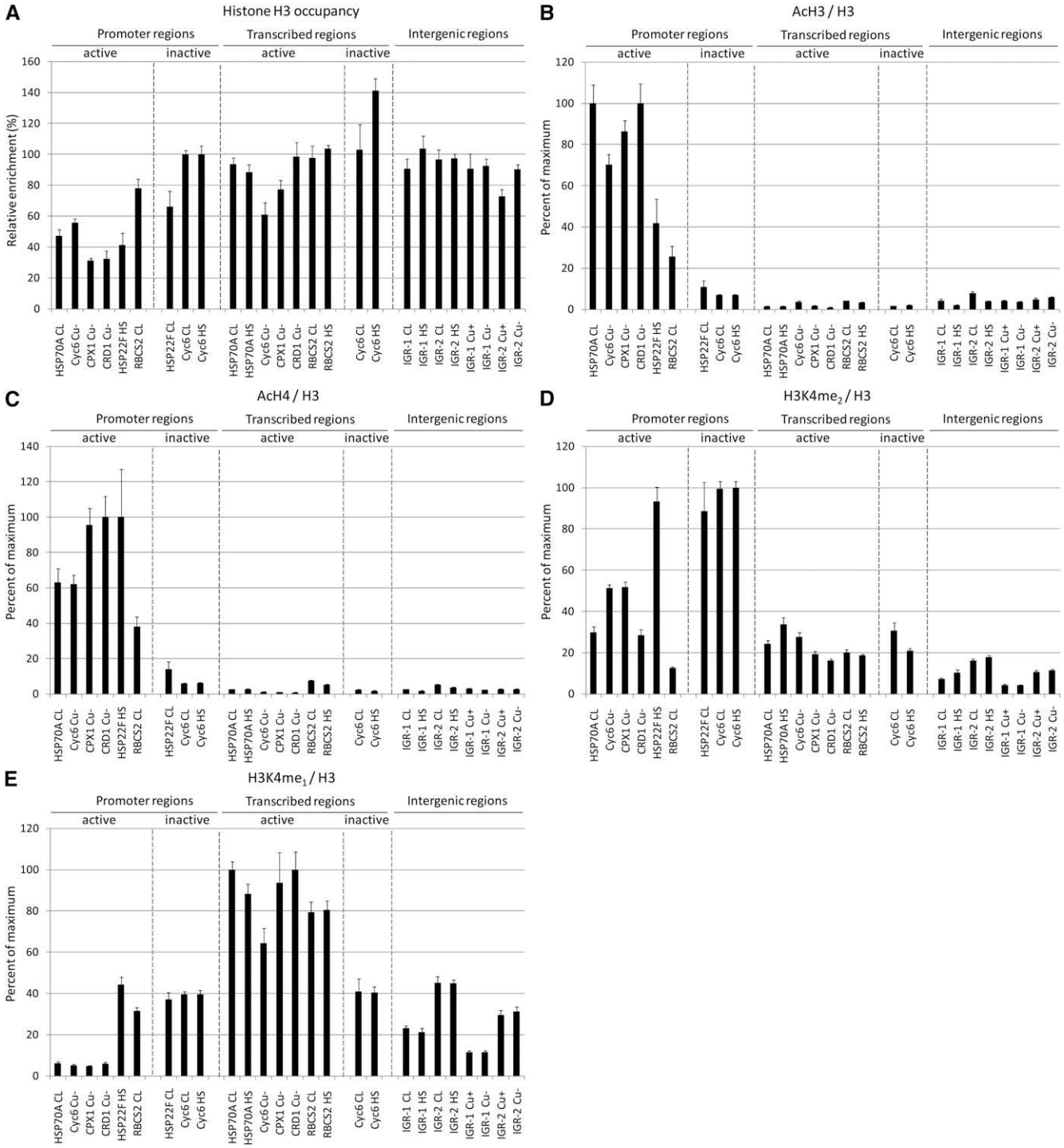

Figure 9. Gene-Wide Overview of the Relative Abundance of Histone Occupancy and Modifications.

ChIP was done on control cells grown under the following conditions: nonstress in copper-replete medium (CL or Cu+), 30 min heat shock (HS), and medium depleted from copper (Cu−). ChIP was done using antibodies against the unmodified C terminus of histone H3 **(A)**, acetylated Lys-9 and -14 of histone H3 **(B)**, acetylated Lys-5, -8, -12, and -16 of histone H4 **(C)**, dimethylation of Lys-4 at histone H3 ($H3K4me_2$) **(D)**, and monomethylation of Lys-4 at histone H3 ($H3K4me_1$) **(E)**. Fragments corresponding to transcribed regions shown in Figure 2 and intergenic regions separating genes au5.g14265_t1/*P23* (IGR-1) and *RBCS2*/au5.g9204_t1 (IGR-2) were amplified by qPCR. The enrichment relative to 10% input DNA was calculated and normalized to the values obtained for the *CYC6* promoter (heat stress experiments) or the *RBCS2* promoter (copper depletion experiments). The data on the promoter regions correspond to that shown in Figures 4 and 7. In case of ChIP analysis with antibodies against modified histones, an additional

A remarkable property of the *HSP70A* promoter is that in a transgene setting it strongly increases the likelihood that a promoter fused downstream becomes active (Schroda et al., 2000, 2002). This effect is dependent on the presence of HSEs within the *HSP70A* promoter, suggesting that it is mediated by HSFs (Lodha et al., 2008). As the constitutively high acetylation levels at the *HSP70A* promoter depend on HSF1, it is tempting to speculate that in the transgene setting the activation of downstream promoters is mediated by histone acetyltransferase activities recruited by HSF1. In turn, the constitutively high acetylation levels at the *CRD1* promoter suggest that like the *HSP70A* promoter it may also be capable of activating neighboring transgenic promoters.

Levels of H3K4 mono- and dimethylation declined in a CRR1-dependent manner at the *CYC6*, *CPX1*, and *CRD1* promoters (Figures 7D, 7E, and 10). Hence, CRR1 appears to recruit histone demethylase activities to its target promoters. Alternatively, CRR1 may recruit histone methyltransferase activities that convert mono- and dimethylated H3 to the trimethylated state. As H3K4 monomethylation in *Chlamydomonas* was shown to be linked to inactive chromatin (van Dijk et al., 2005) and H3K4 trimethylation is widely accepted as a typical mark of active euchromatin (Lachner and Jenuwein, 2002; Santos-Rosa et al., 2002), we favor the latter scenario. In contrast with the copper-responsive promoters, induction of the *HSP22F* promoter was not accompanied with a decline of H3K4 mono- and dimethylation levels (because of the low nucleosome occupancy at the *HSP70A* promoter after heat shock, we cannot draw any conclusions on the methylation state of nucleosomes at that promoter) (Figures 4D, 4E, and 10). In contrast with growth under copper-deficient conditions, cells experienced heat shock only for 30 min. Hence, it is possible that remodeling of the H3K4 methylation state proceeds more slowly than that of the H3/4 acetylation state. In consequence, the acetylation state of a nucleosome appears to be directly connected with promoter activation, while the H3K4 methylation state, as suggested previously (Ng et al., 2003), may serve a memory function to mark promoters that have been active for a certain time. Accordingly, yeast mutants defective in the Set1 and Set2 methyltransferases, catalyzing methylation of histones H3K4 and H3K36, respectively, were hardly impaired in the transcriptional output of the *HSP82* gene (Kremer and Gross, 2009).

Nucleosome Displacement by Activated HSF1 and CRR1 Transcription Factors

Both ChIP and FAIRE analyses revealed that during copper starvation and heat shock, histone occupancy at the copper-responsive promoters and at the *HSP22F* promoter declined in a CRR1- and HSF1-dependent manner, respectively (Figures 4A, 7A, 8, and 10; see Supplemental Figure 6 online). As there is a good correlation between high levels of histone H3/4 acetylation and histone loss at these promoters, it appears that binding of activated CRR1 or HSF1 mediates histone acetylation, thus facilitating histone eviction. This conclusion is supported by a time-course experiment, where HSF1 binding, nucleosome occupancy, H3/4 acetylation, and transcription from the *HSP22F* promoter were monitored within the first 10 min after exposure of cells to heat stress (Figure 5; see Supplemental Figure 6A online). The results indicate the following sequence of events: within the first 30 s after onset of heat stress, HSF1 is activated, binds to the *HSP22F* promoter, and already mediates acetylation of histone H4. Within 60 s after temperature shift, acetylation of H3 and H4 strongly increases, which coincides with nucleosome eviction. Higher levels of *HSP22F* transcripts are detected only 2 min after onset of heat stress, thus indicating that chromatin remodeling at the *HSP22F* promoter most likely is a prerequisite and not a consequence of transcription. Our data agree very well with observations made at the yeast *HSP82* promoter: there, nucleosome occupancy declines drastically within the first 60 s after onset of heat stress and is preceded by a burst of acetylation of histones H2A, H3, and H4 (Zhao et al., 2005). A correlation between histone acetylation and nucleosome loss was demonstrated previously also at the yeast *PHO5*, *SSA4*, and *HSP12* promoters (Reinke and Hörz, 2003; Erkina and Erkine, 2006), at the viral *HTLV-1* promoter in human cells (Sharma and Nyborg, 2008), or at the *Arabidopsis thaliana HSP18.2* promoter (Kodama et al., 2007).

However, we observed that high levels of histone acetylation do not necessarily always correlate with low histone occupancy. For example, H3/4 acetylation levels under nonstress conditions were higher at the *RBCS2* promoter than at the *HSP22F* promoter, but nucleosome occupancy at *HSP22F* was lower than at *RBCS2* (Figures 4A to 4C). Moreover, levels of H3 acetylation at the *HSP70A* promoter were lower in HSF1-underexpressing strains than in the control strain, but these lower acetylation levels were not accompanied by reduced nucleosome occupancy.

Interestingly, the most dramatic nucleosome loss among the promoters studied here, as detected by ChIP and FAIRE, was observed at the *HSP70A* promoter during heat shock (Figures 4A, 8A, and 10). This loss appeared to be HSF1 independent but also may have been mediated by residual HSF1 in HSF1-underexpressing cells (Figure 3). The evidence for strong chromatin remodeling at the *HSP70A* promoter during heat shock, which was obtained by both ChIP and FAIRE experiments, corroborates previous results obtained from micrococcal nuclease digestion studies (Lodha and Schroda, 2005). In that set of experiments, the *HSP70A* promoter under nonstress conditions was found to be embedded into a nucleosome array, which was strongly perturbed by heat shock.

Figure 9. (continued).

normalization was necessary due to different levels of modification within control promoters (*RBCS2* and *CYC6*) that lead to different absolute values between the copper starvation response data set and the heat shock data set. Therefore, the maximum value of each data set was set to 100%. Error bars indicate standard errors of the mean of two biological replicates, each analyzed in triplicate.

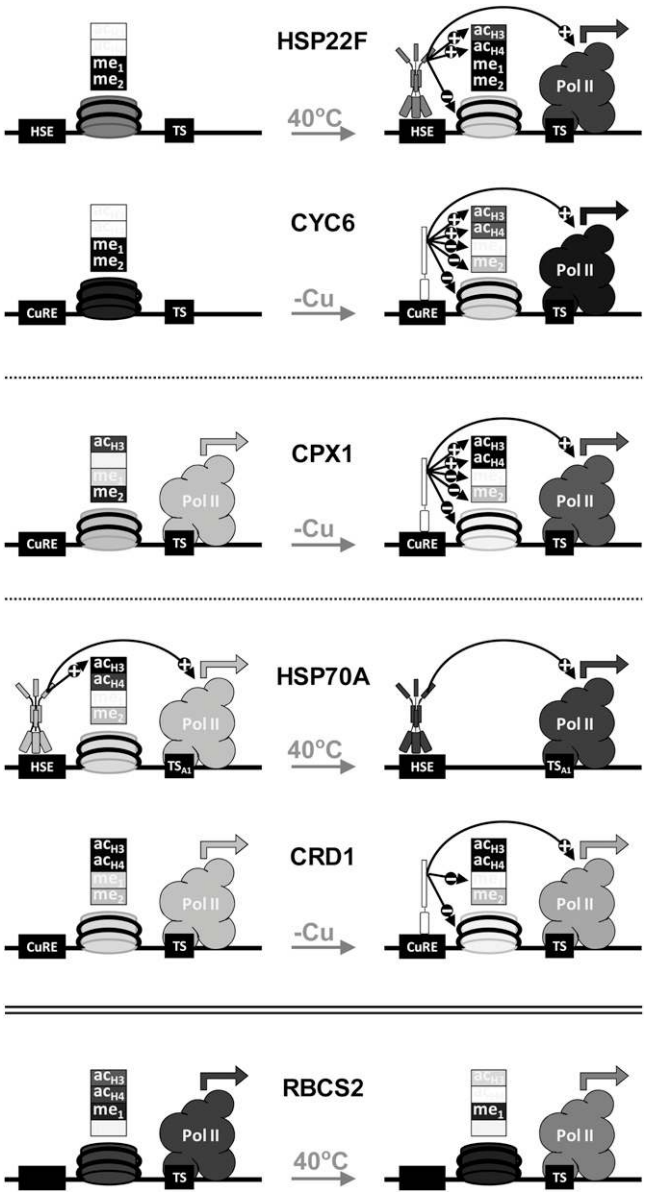

Figure 10. Schematic Description of How Transcription Factors Affect Chromatin State and Activity of the Promoters Studied.

Promoters are schematically depicted by a transcription factor binding site, one nucleosome, and the transcriptional start site (TS). Histone modifications are given on top of the nucleosome, where ac_{H3} stands for acetylation at H3K9 and H3K14; ac_{H4} for acetylation at H4K5, H4K8, H4K12, and H4K16; me_1 for H3K4 monomethylation; and me_2 for H3K4 dimethylation. HSF1 is shown as constitutive trimer, CRR1 as monomer, and polymerase II as multiprotein complex. The darker the symbols for proteins and modifications are drawn, the higher their levels under the respective condition. As we have no data on the occupancy of the CuREs by CRR1, the latter is drawn in white.

Chlamydomonas Promoter Categories Based on Their Chromatin State

Based on their activation by chromatin remodeling, we may place the six promoters analyzed here into four categories (Figure 10): the *CYC6* and *HSP22F* promoters belong to the first category. Under nonstress or copper-replete conditions, these promoters are inactive. The inactive state is mediated by a closed chromatin structure as judged from high nucleosome occupancy, low levels of histone H3/4 acetylation, and high levels of histone H3K4 mono- and dimethylation. HSF1 and CRR1 transcription factors that are activated by heat stress and copper deprivation, respectively, mediate an opening of the chromatin structure at the promoters that is characterized by reduced nucleosome occupancy, high levels of histone H3/4 acetylation, and, presumably only after prolonged activation, reduced levels of histone H3K4 mono- and dimethylation. Moreover, activated HSF1 and CRR1 transcription factors mediate transcription initiation/elongation and, thus, high level transcription of the *HSP22F* and *CYC6* genes.

The *HSP70A* and *CRD1* promoters belong to the second category. They are constitutively in an open chromatin state, as judged from low nucleosome occupancy, high levels of histone H3/4 acetylation, and low levels of histone H3/K4 mono- and dimethylation. Although the chromatin state of the noninduced *HSP70A* and *CRD1* promoters resembles that of the induced *CYC6* promoter, the *HSP70A* and *CRD1* genes under nonstress and copper-replete conditions are only weakly expressed (von Gromoff et al., 1989; Moseley et al., 2000). Apparently, high-level expression under heat stress and copper deprivation conditions requires that the activated HSF1 and CRR1 transcription factors enhance transcription initiation/elongation. At least activated CRR1 also mediates further reduction of nucleosome occupancy. In case of the *HSP70A* promoter, the open chromatin state and basal expression is mediated to a large part by preloaded HSF1, whereas at the *CRD1* promoter it is mediated by an unknown activator.

The *CPX1* promoter belongs to a third category that represents an intermediate between the *HSP22F*/*CYC6* and *HSP70A*/*CRD1* promoter categories in that it has a partially open chromatin structure under noninducing conditions. The latter is characterized by intermediate levels of nucleosome occupancy, high levels of histone H3 acetylation and H3K4 dimethylation, but low levels of histone H4 acetylation and H3K4 monomethylation. Similar to the fully opened *HSP70A* and *CRD1* promoters, the partially opened chromatin state at the *CPX1* promoter allows for low level expression of the *CPX1* gene (Quinn et al., 1999). Thus, *HSP70A*, *CRD1*, and *CPX1* promoters are poised for full transcriptional activation. The fully opened chromatin state at the *CPX1* promoter, mediated by activated CRR1 under copper-deprived conditions and leading to high level expression of the *CPX1* gene, resembles exactly that observed at the *CYC6* promoter.

A fourth category is represented by the *RBCS2* promoter, which is constitutively active and drives constitutive high-level expression of the *RBCS2* gene (Goldschmidt-Clermont and Rahire, 1986). A constitutively active chromatin state at the *RBCS2* promoter is suggested by high levels of histone H3/4 acetylation and low levels of H3K4 dimethylation. However, the *RBCS2* promoter also exhibits high levels of nucleosome

occupancy and H3K4 monomethylation, which rather are characteristic for inactive chromatin. Heat shock leads to a closed chromatin structure, as levels of histone H3/4 acetylation strongly decrease and nucleosome occupancy increases. These results suggested reduced activity of the *RBCS2* promoter under heat stress conditions, which indeed was observed previously for *RBCS2* promoter driven transgenes that are much more weakly expressed than the endogenous *RBCS2* gene (Schroda et al., 2002). Expression levels also of other *Chlamydomonas* genes were observed to decline during heat stress (Dorn et al., 2010). This response might be part of a global, heat shock–induced loss of histone acetylation, which was first observed long ago in *Drosophila melanogaster* (Arrigo, 1983). In contrast with what was reported from a recent study in mammalian cell cultures (Fritah et al., 2009), this effect appears not to depend on HSF1 in *Chlamydomonas*.

In summary, *Chlamydomonas* adjusts gene expression levels in response to changes in environmental conditions by specific transcription factors, such as HSF1 and CRR1 that individually remodel chromatin structure at their target genes, but also by yet unknown factors that appear to generally remodel the chromatin state of many promoters. The most important mark indicative of open chromatin and transcriptionally active promoters appears to be histone acetylation: basal activity of promoters was observed only when at least histone H3 carried high acetylation levels and strong activity was observed only when both histones H3 and H4 were acetylated at high levels. Moreover, histone acetylation preceded nucleosome eviction. By contrast, levels of nucleosome occupancy, H3K4 monomethylation, or H3K4 dimethylation appeared not to have a crucial influence on promoter activity.

The Gene-Wide Distribution of Histone Marks in *Chlamydomonas* versus Yeast

Nucleosome occupancy and histone modifications were determined at a genome-wide scale in yeast by ChIP-on-chip assays (Bernstein et al., 2004; Lee et al., 2004, 2007; Pokholok et al., 2005). When compared with these yeast studies, the glimpse we obtained here by examining selected regions in the *Chlamydomonas* genome suggests similar, but also distinct, features. Similar to yeast, nucleosome occupancy in *Chlamydomonas* in general was low at active promoters and high in transcribed regions (Figures 9 and 10). Moreover, histone H3/4 acetylation was high at promoters of active genes and low at inactive promoters and transcribed and intergenic regions. Furthermore, H3K4 monomethylation was generally low at active promoters and high toward the 3′ end of transcribed regions. Finally, H3K4 dimethylation appeared to be higher at 5′ regions of inactive/weakly transcribed genes compared with actively transcribed genes, which correlated with the notion derived from studies on metazoans that H3K4 dimethylation may mark regions of poised, inactive genes (Schneider et al., 2004; Bernstein et al., 2005; Sims and Reinberg, 2006).

In contrast with what has been observed for yeast, where nucleosome occupancy is low at intergenic regions, we observed high nucleosome occupancy at two intergenic regions (Figure 9). Also, in human cells, nucleosome occupancy appears to be more or less evenly distributed, but contrary to what has been observed for yeast and now *Chlamydomonas*, histones are not particularly depleted at promoter regions (Bernstein et al., 2005). Hence, there appear to be organism-specific differences in histone occupancy and modifications, which can only be elucidated in depth by ChIP-on-chip or ChIP-seq approaches. As the chromatin structure of *Chlamydomonas* appears to be of particularly repressive nature in that nucleosomes exhibit overall low levels of acetylation and high levels of H3K4 monomethylation (Waterborg et al., 1995; van Dijk et al., 2005), it will be of special interest to investigate chromatin structure at a genome-wide level in *Chlamydomonas*.

METHODS

Strains and Cultivation Conditions

To generate strains for investigating the heat shock response, *Chlamydomonas reinhardtii* strain cw15–325 (cw_d, mt^+, *arg7*$^-$; kindly provided by R. Matagne, University of Liège, Belgium) was transformed with pCB412 (containing only the wild-type *ARG7* gene; control strain), pMS418 (containing *ARG7* and an *HSF1*-RNAi construct), and pMS540 (containing *ARG7* and an *HSF1*-amiRNA construct) as described previously (Schulz-Raffelt et al., 2007; Schmollinger et al., 2010). Arg prototrophic transformants were screened for thermosensitivity by exposing cells on agar plates three times within 48 h to a 1-h heat shock by floating plates in a water bath prewarmed to 40°C. To generate strains for investigating the copper response, strain CC3960 (*crr1-2*, *arg7*$^-$; kindly provided by S. Merchant, UCLA, CA) was transformed with plasmid pARG7.8 (Debuchy et al., 1989) or cotransformed with pARG7.8 and pCRR1F1B6 (*CRR1*$^+$ control strain) as described previously (Kropat et al., 2005). Strains were grown mixotrophically to a density of 4 to 7×10^6 cells/mL in Tris-acetate-phosphate medium (Harris, 2008) on a rotary shaker at 24°C and $\sim$30 $\mu E\ m^{-2}\ s^{-1}$. For heat shock experiments, cells were pelleted by a 4-min centrifugation at 24°C and 2704*g*, resuspended in Tris-acetate-phosphate medium prewarmed to 40°C, and incubated under agitation in a water bath at 40°C and $\sim$30 $\mu E\ m^{-2}\ s^{-1}$ for 30 min. Prior to harvest, ice was added to the cells. Copper depletion experiments were performed as described previously (Quinn and Merchant, 1998).

Protein Extraction, Immunodetection, RNA Extraction, and qRT-PCR

Protein extraction and immunoblot analyses were done as described previously (Liu et al., 2005). RNA was isolated from $\sim 10^8$ cells with the TRIzol reagent (Invitrogen) using the manufacturer's protocol except for the last steps: before RNA precipitation, two additional chloroform/isoamyl alcohol (24:1) extractions were performed. A DNase digest was done using RNase-free Turbo DNase (Ambion). The quality of the RNA preparations was estimated by agarose gel electrophoresis, and RNA concentration and purity were determined spectrophotometrically (NanoDrop-1000). cDNA synthesis was performed using the MULV reverse transcriptase (Promega), deoxynucleotide triphosphate, and oligo-d(T)18 primers. Primers for qRT-PCRs were selected based on $\geq$90% primer efficiency, a single melt curve, a single band on a 1.5% agarose gel, and on the correct sequence of the amplicon. They are listed in Supplemental Table 1 online. qRT-PCR was performed using the StepOnePlus RT-PCR system (Applied Biosystems) and the Maxima SYBR Green kit from Fermentas. Each reaction contained the vendor's master mix, 200 nM of each primer, and cDNA corresponding to 10 ng input RNA in the reverse transcriptase reaction. The reaction conditions were as follows: 95°C for 10 min, followed by cycles of 95°C for 15 s and 65°C for 60 s, up to a total of 40 cycles. Primer efficiencies and amplicon sizes for all eight targets are listed in Supplemental Figure 3B online. Controls without template or reverse transcriptase were always included.

ChIP

A total of 10^9 cells that were grown under nonstress conditions and heat shocked for 30 min or grown under copper-replete and copper deprivation conditions were harvested by a 2-min centrifugation at 4°C and 3220*g*. To cross-link protein–DNA interactions, cells were resuspended in 10 mL freshly prepared cross-linking buffer (20 mM HEPES-KOH, pH 7.6, 80 mM KCl, and 0.35% formaldehyde) and incubated for 10 min at 24°C. Cross-linking was quenched by the addition of Gly at a final concentration of 125 mM and further incubation for 5 min at 24°C. Cells were collected by a 2-min centrifugation at 4°C and 3220*g*, washed twice with 1 mL 20 mM HEPES-KOH, pH 7.6, and 80 mM KCl, and lysed by the addition of 400 μL lysis buffer (1% SDS, 10 mM EDTA, 50 mM Tris-HCl, pH 8.0, and 0.25× protease inhibitor cocktail [Roche]). Cells were sonicated on ice using a BANDELIN Sonopuls HD 2070 sonicator with sonication tip MS 73 (55% output control and 60% duty cycle) to gain an average DNA fragment size of ~200 bp. Sonication efficiency was verified for each sample by agarose gel electrophoresis. ChIP was performed with aliquots corresponding to $\sim 2 \times 10^7$ cells that were diluted 1/10 with ChIP buffer (1.1% Triton X-100, 1.2 mM EDTA, 167 mM NaCl, and 16.7 mM Tris-HCl, pH 8) and supplemented with BSA and sonicated λ-DNA at final concentrations of 100 and 1 μg/mL, respectively. Antibodies specific for the following epitopes were used: histone H3 (5 μL; Abcam ab1791); diacetyl H3K9 and H3K14 (10 μL; Upstate 06-599); tetra-acetyl H4K5, H4K8, H4K12, and H4K16 (10 μL; Upstate 06-866); monomethylated H3K4 (5 μL; Abcam ab8895); dimethylated H3K4 (10 μL; Upstate 07-030); HSF1 (40 μL; affinity purified from rabbit antiserum; Schulz-Raffelt et al., 2007); vesicle-inducing protein in plastids 2 (VIPP2) (40 μL; affinity purified from rabbit antiserum, used as mock control). Affinity purification was done as described previously (Willmund and Schroda, 2005). Antibody-protein/DNA complexes were allowed to form during a 1-h incubation at 4°C, were complexed with 6 mg preswollen protein A Sepharose beads (Sigma-Aldrich) during a 2-h incubation at 4°C, and precipitated by a 20-s centrifugation at 16,000*g*. Sepharose beads were washed once with washing buffer 1 (0.1% SDS, 1% Triton X-100, and 2 mM EDTA, pH 8) containing 150 mM NaCl, once with washing buffer 1 containing 500 mM NaCl, once with washing buffer 2 (250 mM LiCl, 1% Nonidet P-40, 1% Na-deoxycholate, 1 mM EDTA, and 10 mM Tris-HCl, pH 8), and twice with TE (1 mM EDTA and 10 mM Tris-HCl, pH 8). Protein-DNA complexes were eluted by incubating twice for 15 min at 65°C in elution buffer (1% SDS and 0.1 M $NaHCO_3$), and cross-links were reverted by an overnight incubation at 65°C after addition of NaCl to a final concentration of 0.5 M. Proteins were digested by incubating for 1 h at 55°C after the addition of proteinase K (3.5 μg/mL), EDTA (8 mM), and Tris-HCl, pH 8.0 (32 mM). DNA was extracted once with phenol/chloroform/isoamyl alcohol (25:24:1), once with chloroform/isoamyl alcohol (24:1), and precipitated by incubation with 2 volumes of ethanol after addition of 0.3 M Na-acetate, pH 5.2, and 10 μg/mL glycogen for 3 h at −20°C. Precipitated DNA was collected by a 20-min centrifugation at 4°C and 16,000*g*, washed with 70% ethanol, and air-dried and resuspended in TE; 1/40th of the precipitated DNA was used for qPCR using the same settings as for qRT-PCR (see above). Controls where template was omitted or derived from ChIP using an affinity-purified antibody against VIPP2 (mock control) were always included. Signals for individual gene regions were normalized against 10% input DNA and then to the corresponding signal derived from the *CYC6* promoter (heat shock) or from the *RBCS2* promoter (copper depletion), which showed no changes after the respective treatment (see Supplemental Figure 5 online). Primers used for qPCR are listed in Supplemental Table 2 online.

FAIRE

A total of 10^9 cells that were grown under nonstress conditions and heat shocked for 30 min or grown under copper-replete and copper deprivation conditions were harvested by a 2-min centrifugation at 4°C and 3220*g*. Cross-linking of DNA–protein interactions was performed exactly as described above for the ChIP Protocol. Cells were sonicated on ice using a BANDELIN Sonopuls HD 2070 sonicator with sonication tip MS 73 (55% output control and 60% duty cycle) to give an average DNA fragment size of ~200 bp. Sonication efficiency was verified for each sample by agarose gel electrophoresis. FAIRE was performed with aliquots corresponding to $\sim 2 \times 10^7$ cells. DNA was extracted once with phenol/chloroform/isoamyl alcohol (25:24:1) and twice with chloroform/isoamyl alcohol (24:1) and precipitated by incubation with 2 volumes of ethanol after addition of 0.3 M Na-acetate, pH 5.2, for 4 h at −20°C. Precipitated DNA was collected by a 20-min centrifugation at 4°C and 16,000*g*, washed with 70% ethanol, air-dried, and resuspended in TE, pH 8. Resuspended DNA was incubated at 65°C for 10 min; 1/40th of 10% of the precipitated DNA was used for qPCR using the same primer pairs as for ChIP (see above).

Accession Numbers

Accession numbers for all genes investigated in this study are given in Supplemental Tables 1 and 2 online.

Supplemental Data

The following materials are available in the online version of this article.

Supplemental Figure 1. Analysis of HSF1 Target Gene Expression in Different *HSF1*-RNAi and *HSF1*-amiRNA Strains.

Supplemental Figure 2. Test of the Specificity of Affinity-Purified HSF1 Antibodies.

Supplemental Figure 3. Experimental Parameters Underlying Transcript Quantification by qRT-PCR.

Supplemental Figure 4. PCR End Products Amplified on Selected Chromatin Precipitates.

Supplemental Figure 5. Nucleosome Occupancy and Histone Modifications at Promoters *CYC6* and *RBCS2* Remain Unaltered after Heat Shock and Copper Depletion, Respectively.

Supplemental Figure 6. Different Amplicons within the *HSP22F* and *CYC6* Promoters Confirm Results.

Supplemental Table 1. Primers Used for qRT-PCR.

Supplemental Table 2. Primers Used for qPCR on Chromatin Precipitates.

ACKNOWLEDGMENTS

We thank Stephen M. Miller (University of Maryland, Baltimore, MD) and Sabeeha Merchant (University of California, Los Angeles, CA) for stimulating discussions and critical comments on the manuscript. We also thank Francis-André Wollman (Institut de Biologie Physico-Chimique, Paris, France) for the antiserum against CF1β. This work was supported by the Max Planck Society and grants from the Deutsche Forschungsgemeinschaft (Schr 617/4-3) and the Bundesministerium für Bildung und Forschung (Systems Biology Initiative FORSYS, Project *Go*FORSYS).

AUTHOR CONTRIBUTIONS

M.S. and D.S. conceived the project and designed the experiments. D.S. performed and analyzed all qRT-PCR, ChIP, and FAIRE experiments. D.S. and S.S. performed the immunoblotting experiments and the statistical analyses. F.S. contributed to setting up copper starvation

experiments and M.S.R. to setting up the ChIP protocol. M.S. and D.S. wrote the manuscript. All authors contributed to the interpretation of results and edited the manuscript.

Received March 15, 2011; revised May 9, 2011; accepted June 7, 2011; published June 24, 2011.

REFERENCES

Aalfs, J.D., and Kingston, R.E. (2000). What does 'chromatin remodeling' mean? Trends Biochem. Sci. **25:** 548–555.

Arrigo, A.P. (1983). Acetylation and methylation patterns of core histones are modified after heat or arsenite treatment of *Drosophila* tissue culture cells. Nucleic Acids Res. **11:** 1389–1404.

Bernstein, B.E., Kamal, M., Lindblad-Toh, K., Bekiranov, S., Bailey, D.K., Huebert, D.J., McMahon, S., Karlsson, E.K., Kulbokas III, E.J., Gingeras, T.R., Schreiber, S.L., and Lander, E.S. (2005). Genomic maps and comparative analysis of histone modifications in human and mouse. Cell **120:** 169–181.

Bernstein, B.E., Liu, C.L., Humphrey, E.L., Perlstein, E.O., and Schreiber, S.L. (2004). Global nucleosome occupancy in yeast. Genome Biol. **5:** R62.

Couture, J.F., Collazo, E., and Trievel, R.C. (2006). Molecular recognition of histone H3 by the WD40 protein WDR5. Nat. Struct. Mol. Biol. **13:** 698–703.

Debuchy, R., Purton, S., and Rochaix, J.D. (1989). The argininosuccinate lyase gene of *Chlamydomonas reinhardtii*: An important tool for nuclear transformation and for correlating the genetic and molecular maps of the *ARG7* locus. EMBO J. **8:** 2803–2809.

de la Cruz, X., Lois, S., Sánchez-Molina, S., and Martínez-Balbás, M.A. (2005). Do protein motifs read the histone code? Bioessays **27:** 164–175.

Dorn, K.V., Willmund, F., Schwarz, C., Henselmann, C., Pohl, T., Hess, B., Veyel, D., Usadel, B., Friedrich, T., Nickelsen, J., and Schroda, M. (2010). Chloroplast DnaJ-like proteins 3 and 4 (CDJ3/4) from *Chlamydomonas reinhardtii* contain redox-active Fe-S clusters and interact with stromal HSP70B. Biochem. J. **427:** 205–215.

Eriksson, M., Moseley, J.L., Tottey, S., Del Campo, J.A., Quinn, J., Kim, Y., and Merchant, S. (2004). Genetic dissection of nutritional copper signaling in *Chlamydomonas* distinguishes regulatory and target genes. Genetics **168:** 795–807.

Erkina, T.Y., and Erkine, A.M. (2006). Displacement of histones at promoters of *Saccharomyces cerevisiae* heat shock genes is differentially associated with histone H3 acetylation. Mol. Cell. Biol. **26:** 7587–7600.

Erkina, T.Y., Zou, Y., Freeling, S., Vorobyev, V.I., and Erkine, A.M. (2010). Functional interplay between chromatin remodeling complexes RSC, SWI/SNF and ISWI in regulation of yeast heat shock genes. Nucleic Acids Res. **38:** 1441–1449.

Fritah, S., Col, E., Boyault, C., Govin, J., Sadoul, K., Chiocca, S., Christians, E., Khochbin, S., Jolly, C., and Vourc'h, C. (2009). Heat-shock factor 1 controls genome-wide acetylation in heat-shocked cells. Mol. Biol. Cell **20:** 4976–4984.

Giresi, P.G., Kim, J., McDaniell, R.M., Iyer, V.R., and Lieb, J.D. (2007). FAIRE (Formaldehyde-Assisted Isolation of Regulatory Elements) isolates active regulatory elements from human chromatin. Genome Res. **17:** 877–885.

Goldschmidt-Clermont, M., and Rahire, M. (1986). Sequence, evolution and differential expression of the two genes encoding variant small subunits of ribulose bisphosphate carboxylase/oxygenase in *Chlamydomonas reinhardtii.* J. Mol. Biol. **191:** 421–432.

Harris, E.H. (2008). The *Chlamydomonas* Sourcebook: Introduction to *Chlamydomonas* and Its Laboratory Use. (San Diego, CA: Elsevier/Academic Press).

Haslbeck, M. (2002). sHsps and their role in the chaperone network. Cell. Mol. Life Sci. **59:** 1649–1657.

Kodama, Y., Nagaya, S., Shinmyo, A., and Kato, K. (2007). Mapping and characterization of DNase I hypersensitive sites in *Arabidopsis* chromatin. Plant Cell Physiol. **48:** 459–470.

Kouzarides, T. (2007). Chromatin modifications and their function. Cell **128:** 693–705.

Kremer, S.B., and Gross, D.S. (2009). SAGA and Rpd3 chromatin modification complexes dynamically regulate heat shock gene structure and expression. J. Biol. Chem. **284:** 32914–32931.

Krogan, N.J., Dover, J., Wood, A., Schneider, J., Heidt, J., Boateng, M.A., Dean, K., Ryan, O.W., Golshani, A., Johnston, M., Greenblatt, J.F., and Shilatifard, A. (2003). The Paf1 complex is required for histone H3 methylation by COMPASS and Dot1p: Linking transcriptional elongation to histone methylation. Mol. Cell **11:** 721–729.

Kropat, J., Tottey, S., Birkenbihl, R.P., Depège, N., Huijser, P., and Merchant, S. (2005). A regulator of nutritional copper signaling in *Chlamydomonas* is an SBP domain protein that recognizes the GTAC core of copper response element. Proc. Natl. Acad. Sci. USA **102:** 18730–18735.

Lachner, M., and Jenuwein, T. (2002). The many faces of histone lysine methylation. Curr. Opin. Cell Biol. **14:** 286–298.

Lee, C.K., Shibata, Y., Rao, B., Strahl, B.D., and Lieb, J.D. (2004). Evidence for nucleosome depletion at active regulatory regions genome-wide. Nat. Genet. **36:** 900–905.

Lee, J.H., Hübel, A., and Schöffl, F. (1995). Derepression of the activity of genetically engineered heat shock factor causes constitutive synthesis of heat shock proteins and increased thermotolerance in transgenic *Arabidopsis.* Plant J. **8:** 603–612.

Lee, W., Tillo, D., Bray, N., Morse, R.H., Davis, R.W., Hughes, T.R., and Nislow, C. (2007). A high-resolution atlas of nucleosome occupancy in yeast. Nat. Genet. **39:** 1235–1244.

Li, B., Carey, M., and Workman, J.L. (2007). The role of chromatin during transcription. Cell **128:** 707–719.

Li, H., Ilin, S., Wang, W., Duncan, E.M., Wysocka, J., Allis, C.D., and Patel, D.J. (2006). Molecular basis for site-specific read-out of histone H3K4me3 by the BPTF PHD finger of NURF. Nature **442:** 91–95.

Liu, C., Willmund, F., Whitelegge, J.P., Hawat, S., Knapp, B., Lodha, M., and Schroda, M. (2005). J-domain protein CDJ2 and HSP70B are a plastidic chaperone pair that interacts with vesicle-inducing protein in plastids 1. Mol. Biol. Cell **16:** 1165–1177.

Lodha, M., and Schroda, M. (2005). Analysis of chromatin structure in the control regions of the *Chlamydomonas HSP70A* and *RBCS2* genes. Plant Mol. Biol. **59:** 501–513.

Lodha, M., Schulz-Raffelt, M., and Schroda, M. (2008). A new assay for promoter analysis in *Chlamydomonas* reveals roles for heat shock elements and the *TATA* box in *HSP70A* promoter-mediated activation of transgene expression. Eukaryot. Cell **7:** 172–176.

Luger, K. (2003). Structure and dynamic behavior of nucleosomes. Curr. Opin. Genet. Dev. **13:** 127–135.

Merchant, S., and Bogorad, L. (1986). Regulation by copper of the expression of plastocyanin and cytochrome c552 in *Chlamydomonas reinhardi.* Mol. Cell. Biol. **6:** 462–469.

Merchant, S., and Bogorad, L. (1987). Metal ion regulated gene expression: Use of a plastocyanin-less mutant of *Chlamydomonas reinhardtii* to study the Cu(II)-dependent expression of cytochrome c-552. EMBO J. **6:** 2531–2535.

Merchant, S.S., Allen, M.D., Kropat, J., Moseley, J.L., Long, J.C., Tottey, S., and Terauchi, A.M. (2006). Between a rock and a hard place: Trace element nutrition in *Chlamydomonas.* Biochim. Biophys. Acta **1763:** 578–594.

Moseley, J., Quinn, J., Eriksson, M., and Merchant, S. (2000). The *Crd1* gene encodes a putative di-iron enzyme required for photosystem I

accumulation in copper deficiency and hypoxia in *Chlamydomonas reinhardtii.* EMBO J. **19:** 2139–2151.

Müller, F.W., Igloi, G.L., and Beck, C.F. (1992). Structure of a gene encoding heat-shock protein HSP70 from the unicellular alga *Chlamydomonas reinhardtii.* Gene **111:** 165–173.

Ng, H.H., Robert, F., Young, R.A., and Struhl, K. (2003). Targeted recruitment of Set1 histone methylase by elongating Pol II provides a localized mark and memory of recent transcriptional activity. Mol. Cell **11:** 709–719.

Owen, D.J., Ornaghi, P., Yang, J.C., Lowe, N., Evans, P.R., Ballario, P., Neuhaus, D., Filetici, P., and Travers, A.A. (2000). The structural basis for the recognition of acetylated histone H4 by the bromodomain of histone acetyltransferase gcn5p. EMBO J. **19:** 6141–6149.

Pelham, H.R. (1982). A regulatory upstream promoter element in the *Drosophila hsp 70* heat-shock gene. Cell **30:** 517–528.

Peña, P.V., Davrazou, F., Shi, X., Walter, K.L., Verkhusha, V.V., Gozani, O., Zhao, R., and Kutateladze, T.G. (2006). Molecular mechanism of histone H3K4me3 recognition by plant homeodomain of ING2. Nature **442:** 100–103.

Pokholok, D.K., et al. (2005). Genome-wide map of nucleosome acetylation and methylation in yeast. Cell **122:** 517–527.

Quinn, J.M., and Merchant, S. (1995). Two copper-responsive elements associated with the *Chlamydomonas Cyc6* gene function as targets for transcriptional activators. Plant Cell **7:** 623–628.

Quinn, J.M., and Merchant, S. (1998). Copper-responsive gene expression during adaptation to copper deficiency. Methods Enzymol. **297:** 263–279.

Quinn, J.M., Nakamoto, S.S., and Merchant, S. (1999). Induction of coproporphyrinogen oxidase in *Chlamydomonas* chloroplasts occurs via transcriptional regulation of Cpx1 mediated by copper response elements and increased translation from a copper deficiency-specific form of the transcript. J. Biol. Chem. **274:** 14444–14454.

Rabindran, S.K., Haroun, R.I., Clos, J., Wisniewski, J., and Wu, C. (1993). Regulation of heat shock factor trimer formation: Role of a conserved leucine zipper. Science **259:** 230–234.

Reid, J.L., Iyer, V.R., Brown, P.O., and Struhl, K. (2000). Coordinate regulation of yeast ribosomal protein genes is associated with targeted recruitment of Esa1 histone acetylase. Mol. Cell **6:** 1297–1307.

Reinke, H., and Hörz, W. (2003). Histones are first hyperacetylated and then lose contact with the activated PHO5 promoter. Mol. Cell **11:** 1599–1607.

Robert, F., Pokholok, D.K., Hannett, N.M., Rinaldi, N.J., Chandy, M., Rolfe, A., Workman, J.L., Gifford, D.K., and Young, R.A. (2004). Global position and recruitment of HATs and HDACs in the yeast genome. Mol. Cell **16:** 199–209.

Ruthenburg, A.J., Wang, W., Graybosch, D.M., Li, H., Allis, C.D., Patel, D.J., and Verdine, G.L. (2006). Histone H3 recognition and presentation by the WDR5 module of the MLL1 complex. Nat. Struct. Mol. Biol. **13:** 704–712.

Santos-Rosa, H., Schneider, R., Bannister, A.J., Sherriff, J., Bernstein, B.E., Emre, N.C., Schreiber, S.L., Mellor, J., and Kouzarides, T. (2002). Active genes are tri-methylated at K4 of histone H3. Nature **419:** 407–411.

Schmollinger, S., Strenkert, D., and Schroda, M. (2010). An inducible artificial microRNA system for *Chlamydomonas reinhardtii* confirms a key role for heat shock factor 1 in regulating thermotolerance. Curr. Genet. **56:** 383–389.

Schneider, R., Bannister, A.J., Myers, F.A., Thorne, A.W., Crane-Robinson, C., and Kouzarides, T. (2004). Histone H3 lysine 4 methylation patterns in higher eukaryotic genes. Nat. Cell Biol. **6:** 73–77.

Schroda, M., Beck, C.F., and Vallon, O. (2002). Sequence elements within an *HSP70* promoter counteract transcriptional transgene silencing in *Chlamydomonas.* Plant J. **31:** 445–455.

Schroda, M., Blöcker, D., and Beck, C.F. (2000). The *HSP70A* promoter as a tool for the improved expression of transgenes in *Chlamydomonas.* Plant J. **21:** 121–131.

Schroda, M., and Vallon, O. (2008). Chaperones and proteases. In The *Chlamydomonas* Sourcebook: Organellar and Metabolic Processes, 2nd ed, Vol. 2, D.B. Stern, ed (San Diego, CA: Academic Press), pp. 671-729.

Schulz-Raffelt, M., Lodha, M., and Schroda, M. (2007). Heat shock factor 1 is a key regulator of the stress response in *Chlamydomonas.* Plant J. **52:** 286–295.

Sharma, N., and Nyborg, J.K. (2008). The coactivators CBP/p300 and the histone chaperone NAP1 promote transcription-independent nucleosome eviction at the HTLV-1 promoter. Proc. Natl. Acad. Sci. USA **105:** 7959–7963.

Shi, X., et al. (2006). ING2 PHD domain links histone H3 lysine 4 methylation to active gene repression. Nature **442:** 96–99.

Sims III, R.J., and Reinberg, D. (2006). Histone H3 Lys 4 methylation: Caught in a bind? Genes Dev. **20:** 2779–2786.

Sommer, F., Kropat, J., Malasarn, D., Grossoehme, N.E., Chen, X., Giedroc, D.P., and Merchant, S.S. (2010). The CRR1 nutritional copper sensor in *Chlamydomonas* contains two distinct metal-responsive domains. Plant Cell **22:** 4098–4113.

Sorger, P.K., Lewis, M.J., and Pelham, H.R. (1987). Heat shock factor is regulated differently in yeast and HeLa cells. Nature **329:** 81–84.

Sorger, P.K., and Nelson, H.C. (1989). Trimerization of a yeast transcriptional activator via a coiled-coil motif. Cell **59:** 807–813.

Sorger, P.K., and Pelham, H.R. (1988). Yeast heat shock factor is an essential DNA-binding protein that exhibits temperature-dependent phosphorylation. Cell **54:** 855–864.

Tottey, S., Block, M.A., Allen, M., Westergren, T., Albrieux, C., Scheller, H.V., Merchant, S., and Jensen, P.E. (2003). *Arabidopsis* CHL27, located in both envelope and thylakoid membranes, is required for the synthesis of protochlorophyllide. Proc. Natl. Acad. Sci. USA **100:** 16119–16124.

van Dijk, K., Marley, K.E., Jeong, B.R., Xu, J., Hesson, J., Cerny, R.L., Waterborg, J.H., and Cerutti, H. (2005). Monomethyl histone H3 lysine 4 as an epigenetic mark for silenced euchromatin in *Chlamydomonas.* Plant Cell **17:** 2439–2453.

von Gromoff, E.D., Schroda, M., Oster, U., and Beck, C.F. (2006). Identification of a plastid response element that acts as an enhancer within the *Chlamydomonas HSP70A* promoter. Nucleic Acids Res. **34:** 4767–4779.

von Gromoff, E.D., Treier, U., and Beck, C.F. (1989). Three light-inducible heat shock genes of *Chlamydomonas reinhardtii.* Mol. Cell. Biol. **9:** 3911–3918.

Waterborg, J.H., Robertson, A.J., Tatar, D.L., Borza, C.M., and Davie, J.R. (1995). Histones of *Chlamydomonas reinhardtii*. Synthesis, acetylation, and methylation. Plant Physiol. **109:** 393–407.

Willmund, F., and Schroda, M. (2005). HEAT SHOCK PROTEIN 90C is a bona fide Hsp90 that interacts with plastidic HSP70B in *Chlamydomonas reinhardtii.* Plant Physiol. **138:** 2310–2322.

Wood, P.M. (1978). Interchangeable copper and iron proteins in algal photosynthesis. Studies on plastocyanin and cytochrome c-552 in *Chlamydomonas.* Eur. J. Biochem. **87:** 9–19.

Zeng, L., Zhang, Q., Li, S., Plotnikov, A.N., Walsh, M.J., and Zhou, M.M. (2010). Mechanism and regulation of acetylated histone binding by the tandem PHD finger of DPF3b. Nature **466:** 258–262.

Zhang, L., Lohmann, C., Prändl, R., and Schöffl, F. (2003). Heat stress-dependent DNA binding of *Arabidopsis* heat shock transcription factor HSF1 to heat shock gene promoters in *Arabidopsis* suspension culture cells *in vivo.* Biol. Chem. **384:** 959–963.

Zhao, J., Herrera-Diaz, J., and Gross, D.S. (2005). Domain-wide displacement of histones by activated heat shock factor occurs independently of Swi/Snf and is not correlated with RNA polymerase II density. Mol. Cell. Biol. **25:** 8985–8999.